



# Nonlinear $^{40}\text{Ar}/^{39}\text{Ar}$ age systematics along the Gilbert Ridge and Tokelau Seamount Trail and the timing of the Hawaii-Emperor Bend

**Anthony A. P. Koppers**

*Institute of Geophysics and Planetary Physics, Scripps Institution of Oceanography, University of California, San Diego, La Jolla, California 92093-0225, USA*

*Now at College of Oceanic and Atmospheric Sciences, Oregon State University, 104 COAS Administration Building, Corvallis, Oregon 97331-5503, USA (akoppers@coas.oregonstate.edu)*

**Hubert Staudigel**

*Institute of Geophysics and Planetary Physics, Scripps Institution of Oceanography, University of California, San Diego, La Jolla, California 92093-0225, USA*

**Jason Phipps Morgan**

*Department of Earth and Atmospheric Sciences, Cornell University, 4164 Snee Hall, Ithaca, New York 14853, USA*

**Robert A. Duncan**

*College of Oceanic and Atmospheric Sciences, Oregon State University, 104 COAS Administration Building, Corvallis, Oregon 97331-5503, USA*

[1] Over the last three decades the first-order correlation in morphology and orientation of seamount trails has been called upon to support the concept of a “fixed” Pacific hot spot frame of reference and to explain the Hawaii-Emperor bend (HEB) by a dramatic change in Pacific plate motion. In this paper, however, we present  $^{40}\text{Ar}/^{39}\text{Ar}$  ages for the Gilbert Ridge and Tokelau Seamounts (Pacific) that show similar changes or bends in their orientation, but at different geological times, up to 20 Myr earlier than the HEB. Changes in Pacific plate motion alone cannot explain these observations, because these asynchronous bends should have been reflected in the morphology of each of these seamount trails. Together with the lack of (linear) age progressions and inconsistent apparent local plate velocities of 131 and 87 mm/yr, we rule out a fixed hot spot origin for the Gilbert Ridge and Tokelau seamount trails. Instead we invoke secondary or alternate processes to explain the complex age systematics and morphologies in these seamount trails. We propose here that the HEB-type bends in these seamount trails were likely formed by short-term “jerk-like” plate extensions in the studied southwestern region of the Pacific plate, reactivating a preconditioned lithosphere that can be characterized by a complex structure and precursory magmatic impingements. The remarkable differences observed in these colinear seamount trails fundamentally question the existence of HEB-type bends in the formation of Pacific volcanic lineaments. They also show us that applying geometric and morphologic observations alone is insufficient in constraining past plate motions. Nevertheless, the need and search for alternate volcano-tectonic mechanisms offer opportunities to better understand intraplate volcanism in general.



**Components:** 14,459 words, 10 figures, 5 tables.

**Keywords:**  $^{40}\text{Ar}/^{39}\text{Ar}$  geochronology; seamounts; Pacific plate; hot spots; intraplate volcanism; local lithospheric extension.

**Index Terms:** 1115 Geochronology: Radioisotope geochronology; 8415 Volcanology: Intra-plate processes (1033, 3615); 9355 Geographic Location: Pacific Ocean.

**Received** 26 September 2006; **Revised** 1 February 2007; **Accepted** 14 March 2007; **Published** 16 June 2007.

Koppers, A. A. P., H. Staudigel, J. Phipps Morgan, and R. A. Duncan (2007), Nonlinear  $^{40}\text{Ar}/^{39}\text{Ar}$  age systematics along the Gilbert Ridge and Tokelau Seamount Trail and the timing of the Hawaii-Emperor Bend, *Geochem. Geophys. Geosyst.*, 8, Q06L13, doi:10.1029/2006GC001489.

**Theme:** Movement, Dynamics, and Geochemical Evolution of the Hawaiian Hot Spot

**Guest Editors:** T. Davies, R. Duncan, D. Scholl, and J. A. Tarduno

## 1. Introduction

[2] Much of the ongoing debate on plate motion and a frame of reference based on stationary hot spots focuses on the dynamical and geological record of the Hawaiian hot spot. For decades, this hot spot provided the classic example of the “fixed” hot spot, with its well-characterized age progression along a more or less linear volcanic island and seamount trail. The sharp  $60^\circ$  change in the “Hawaii-Emperor Bend” (HEB) has been considered the evidence of a major plate reorganization [Morgan, 1972a; Duncan and Clague, 1985], which most recently was dated at 47 Ma [Sharp and Clague, 2006]. The Hawaii-Emperor volcanic lineament is typically seen as the key to the understanding of all other volcanic lineaments in the Pacific basin, even though it is an end-member in its large volume and longevity [Courtilot *et al.*, 2003; Koppers *et al.*, 2003b].

[3] This role of Hawaii as the archetypal hot spot and as the key to Pacific plate motion has attracted challenging scientific scrutiny. Cande *et al.* [1995] demonstrated that the Hawaii-Emperor hot spot track cannot be reconciled with the fixed hot spot frame of reference derived from Indo-Atlantic seamount trails. Paleomagnetic studies of the Emperor seamounts suggested a  $\sim 15^\circ$  southern shift of the Hawaiian hot spot between 80 and 47 Ma [Tarduno *et al.*, 2003], which also was detected in the changing positions of the paleo-equator as derived by mapping of the maxima in sediment accumulation, reflecting equatorial productivity [Pares and Moore, 2005]. These studies show very clearly that our textbook example of a fixed hot spot cannot be stationary with respect to

the spin axis [Norton, 1995; Koppers *et al.*, 2001; Tarduno *et al.*, 2003]. Questions now arise about the origin of other volcanic lineaments in the Pacific and intraplate volcanism in general. For example, if the HEB was at least partly caused by hot spot motion, does this mean that all other seamount trails with similar trends and bends are caused by the same processes? Can we take into account hot spot motion and still quantitatively describe plate motion with respect to a mantle-based reference frame? Should we consider different types of hot spots? Does the moving hot spot concept explain all intraplate volcanism or do we have to consider alternate models of volcanism related to plate extension?

[4] None of these questions can be answered by studying the Hawaii-Emperor chain alone. It is critical to produce independent evidence and integrate this information with what we know about seamount trails in general. This led us to search for other HEB-type bends in volcanic trails in the Pacific Basin to explore them for their timing and morphological expressions. The most obvious candidate is the Louisville seamount chain, which offers the next-best example of a Pacific seamount trail, because it is also a long-lived and prominent feature that is well-dated and spans the HEB time period [Watts *et al.*, 1988; Koppers *et al.*, 2004]. However, this seamount trail is not useful for an independent age constraint of the HEB, because it shows a broad curvature at its bend [Lonsdale, 1988], even though its minimal  $^{40}\text{Ar}/^{39}\text{Ar}$  age of 46 Ma [Koppers *et al.*, 2004] appears to be coeval with the HEB. The Gilbert Ridge and Tokelau seamount trails are two other volcanic lineaments in the Pacific basin that display HEB-type bends and are located close to one another in the SW

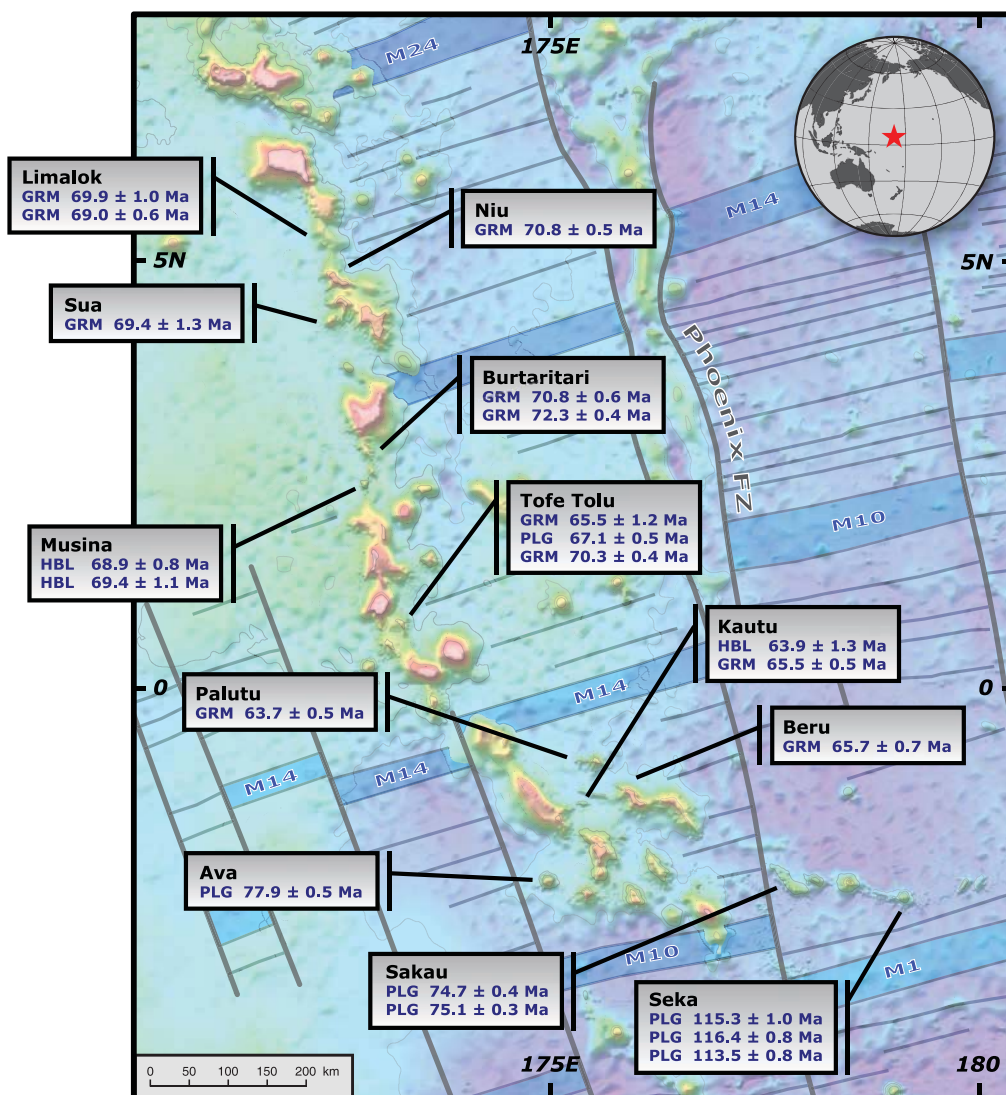


**Figure 1.** Bathymetric maps of the Gilbert Ridge and Tokelau seamount trails. The seafloor magnetic anomalies [Cande and Kent, 1995], some important morphological features, and the fracture zones in the underlying oceanic basement are shown for reference. Changes in orientation (bends) can be recognized in both seamount trails at the equator for the Gilbert Ridge and around 3°S and 9°S for the Tokelau seamount trail. The measured ages (in Ma) and the material types (GRM, groundmass; HBL, hornblende; PLG, plagioclase; BIO, biotite) have been indicated in text boxes. The bathymetric maps are based on a combination of SeaBEAM 2000 multibeam data collected during the Avon Leg 2 cruise on board the R/V *Melville* and are merged with the global predicted bathymetry (v8.2) from *Smith and Sandwell* [1997]. For detailed seamount maps and the underlying data files, we refer to Appendix B, which contains links for each seamount to the Seamount Catalog at the EarthRef.org Web site. Note that the Gilbert Ridge continues into the Ratak Chain in the Marshall Islands (not shown) on the north side of this map, whereas no morphological continuation to the south is evident. The Tokelau Seamounts do not extend to either the north or south side of the shown map.

Pacific (Figure 1). Both trails seem to have formed predominantly during the NNW-trending Emperor stage and have pronounced curvatures at their southern ends, closely resembling the HEB, except that they do not continue far into the Hawaiian stage. Although these seamount trails show sharp

bends in their morphology, the timing of their bends are asynchronous with the HEB, at 67 and 57 Ma, indicating that fixed hot spots and a uniform change in Pacific plate motion cannot explain the formation of the Gilbert Ridge and Tokelau Seamounts [Koppers and Staudigel, 2005]. Their

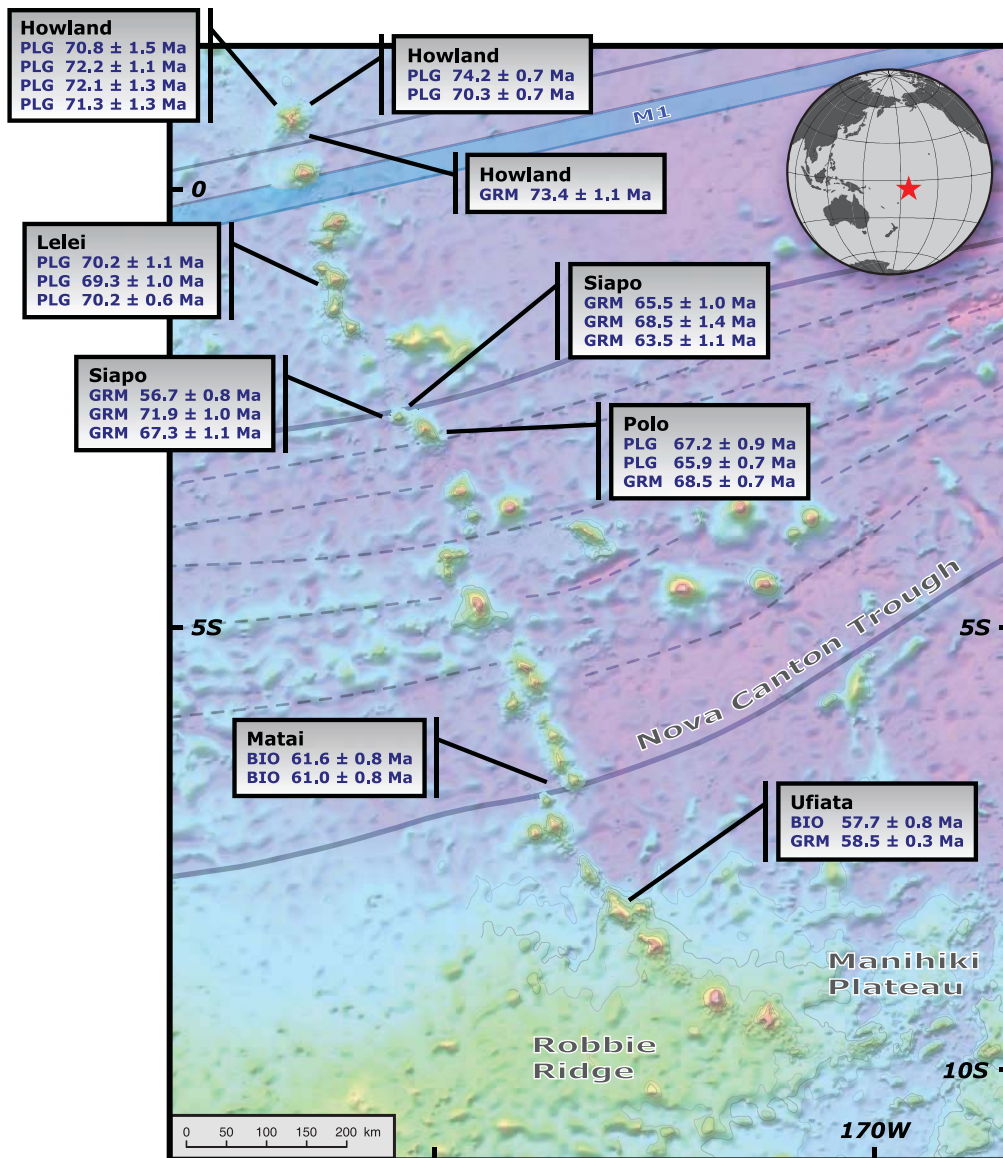
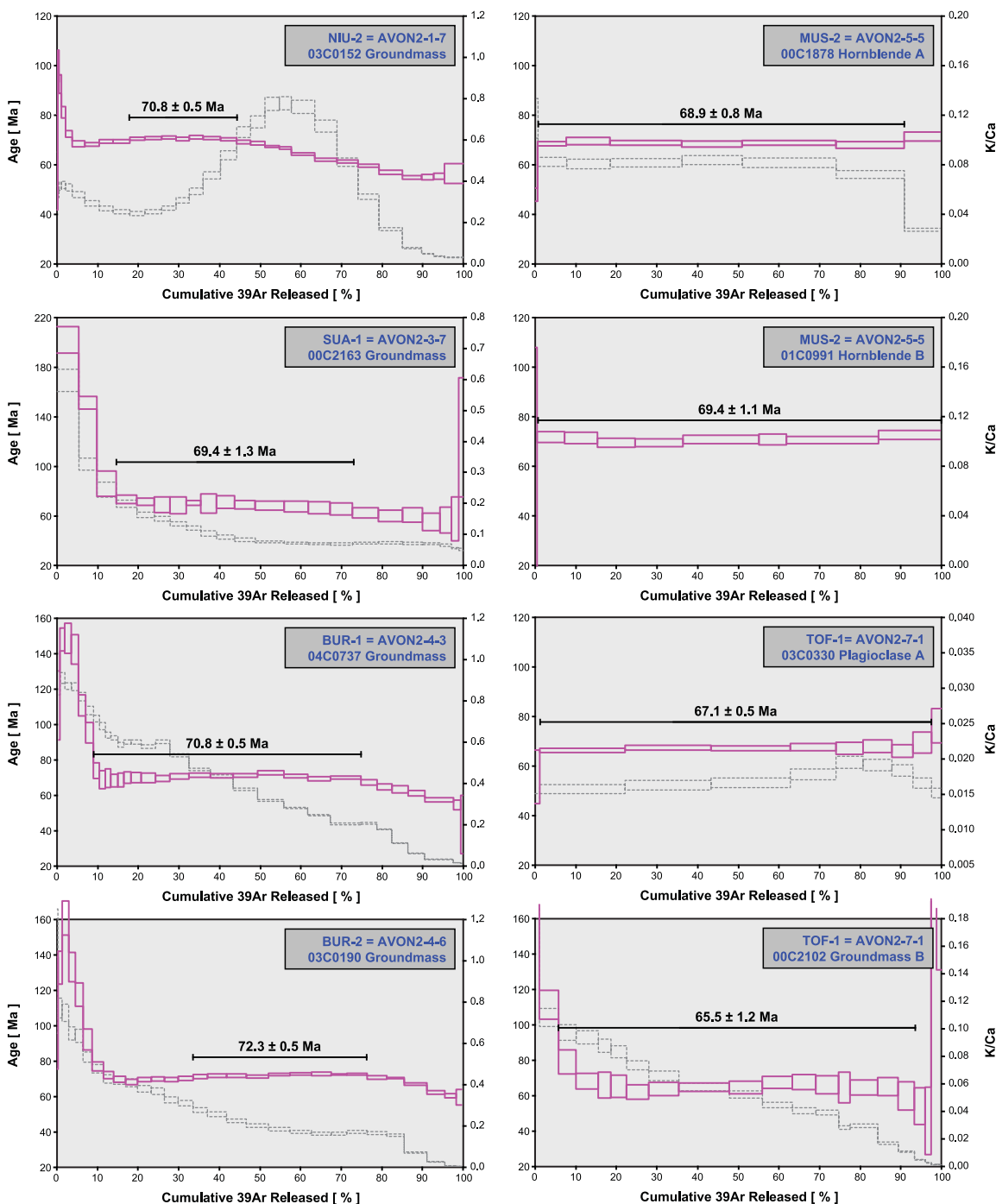


Figure 1. (continued)

bends might not be the envisioned HEB-type features after all.

[5] In this paper, we examine the age distribution and geology of the Gilbert Ridge and Tokelau seamount trails to evaluate alternative models that might explain the above observations. New <sup>40</sup>Ar/<sup>39</sup>Ar age determinations for both seamount trails are presented, giving additional coverage away from the HEB-type bends [Koppers and Staudigel, 2005] and including seamounts that are significantly older than 70 Ma, predating the bulk of intraplate volcanism forming these volcanic trails. In particular, we investigate the possibilities of inter-hot spot motion, short-lived hot spot vol-

canism and rejuvenated volcanism caused by lithospheric extension. We also explore the possible continuation of the Gilbert Ridge into the Tuvalu-Ellice seamount trail that is located southward and merges with the Samoan seamounts, as originally suggested by Morgan [1972b]. Each of the above scenarios has aspects that may explain our new age determinations. However, in this paper, we conclude that the HEB-type bends in the Gilbert Ridge and Tokelau seamount trails were formed by short-term “jerk-like” plate extensions in the Pacific plate, which locally has been preconditioned by the presence of older seamount trails and by the



**Figure 2.** High-resolution incremental heating <sup>40</sup>Ar/<sup>39</sup>Ar age spectra for Gilbert Ridge and Tokelau seamount trail basalts. The reported <sup>40</sup>Ar/<sup>39</sup>Ar ages are weighted age estimates with errors reported on the 95% confidence level, including 0.3–0.4% standard deviations in the J-value. All samples were monitored against FCT-3 biotite (28.04 ± 0.18 Ma, 1σ) as calibrated by *Renne et al.* [1998]. The measured K/Ca ratios are displayed as dashed gray lines. Data are listed in Tables 2a and 2b, and ArArCALC age calculation files can be downloaded from the EarthRef.org Digital Archive (ERDA) as described in Appendix A.

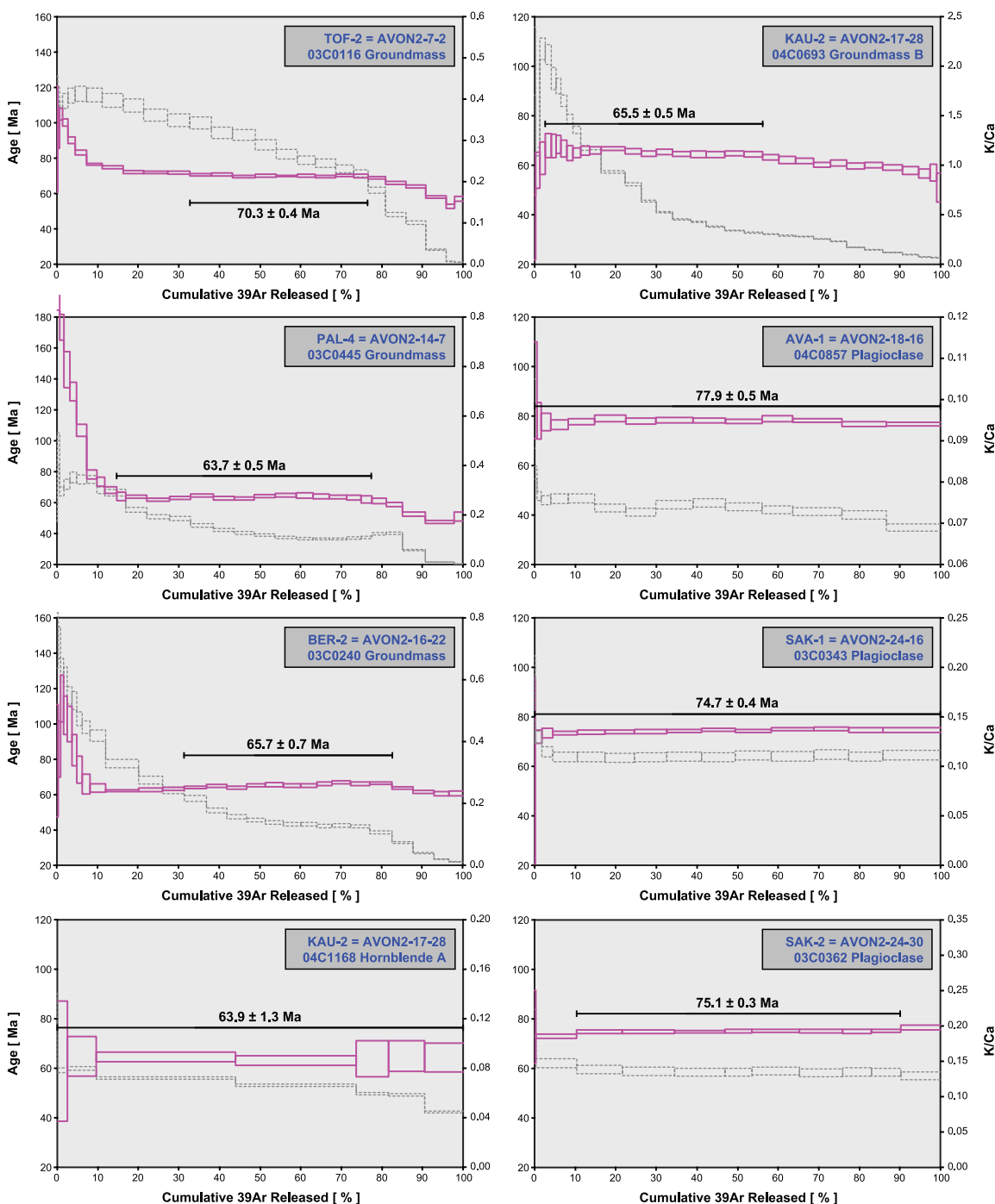


Figure 2. (continued)

intrusion of basaltic sills during the emplacement of the Ontong Java plateau.

## 2. <sup>40</sup>Ar/<sup>39</sup>Ar Dating Techniques

[6] In total we performed 43 new <sup>40</sup>Ar/<sup>39</sup>Ar incremental heating analyses on 35 samples from

17 seamounts or guyots of the Gilbert Ridge and Tokelau Seamounts in the Mid-Pacific. The results of these incremental heating experiments are displayed in age plateau and isochron diagrams in Figures 2 and 3 respectively. Seamount locations and a summary of the <sup>40</sup>Ar/<sup>39</sup>Ar ages are listed in Tables 1, 2a, and 2b. The measurement data can be

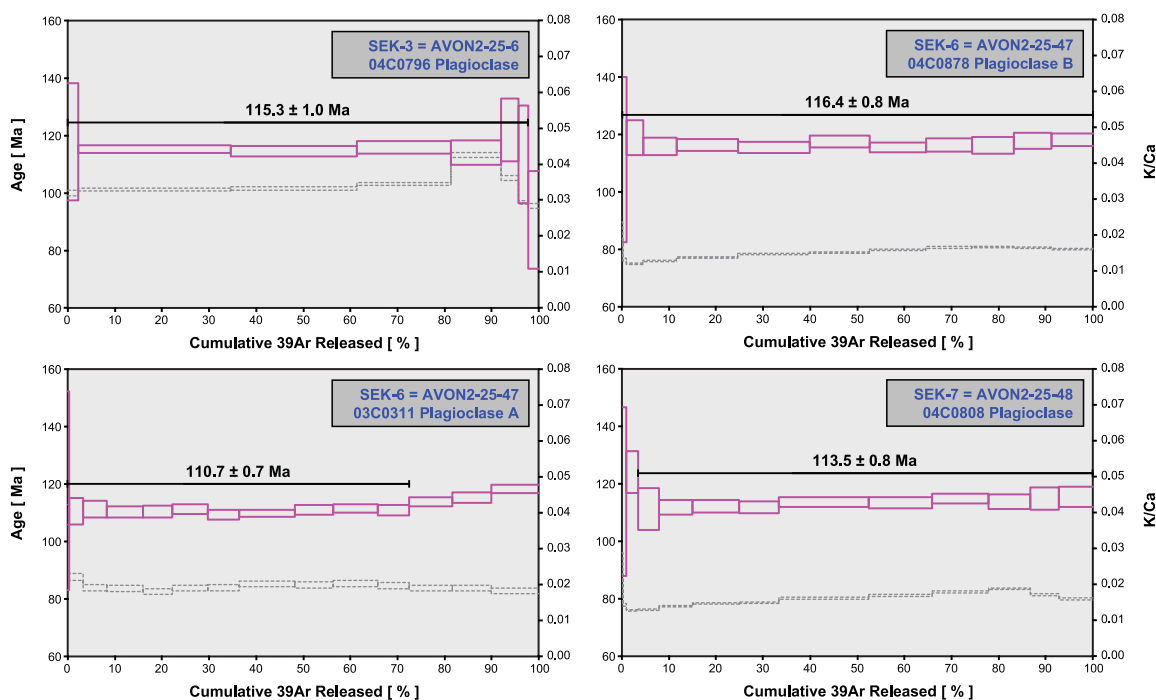


Figure 2. (continued)

downloaded from the EarthRef.org Digital Archive (ERDA) as detailed in Appendix A.

[7] The <sup>40</sup>Ar/<sup>39</sup>Ar incremental heating age determinations were performed on crystalline groundmass separates (250–500 μm) and plagioclase, hornblende and biotite mineral separates using a continuous, 10W CO<sub>2</sub> laser probe combined with a MAP-215/50 mass spectrometer at Oregon State University. Sample preparation and acid leaching procedures are described by *Koppers et al.* [2000]. The mass spectrometer is a 90° sector instrument with a Nier-type source with an all-metal gas extraction system. It has an electron multiplier for high sensitivity and an electrostatic analyzer with adjustable collector slit for an effective resolution (~600) of Ar peaks from small hydrocarbon peaks. Irradiated groundmass samples were loaded into Cu-planchettes designed with a variety of pans that hold up to 50 mg of material, which are then pumped within a sample chamber fitted with a ZnSe window that is transparent to the CO<sub>2</sub> laser wavelength. Software allows for scanning across samples in a preset pattern with a defocused beam, to evenly heat the geological material. Gas cleanup was accomplished with a series of Zr-Al getters. All ages were calculated relative to the flux monitor standard FCT-3 biotite (28.04 ± 0.18 Ma, 1σ [Renne et al., 1994]) and calculated using the corrected *Steiger and Jäger* [1977] decay constant

of  $5.530 \pm 0.097 \times 10^{-10}$  1/yr (2σ) as reported by *Min et al.* [2000]. For a detailed description of the analytical facility and the constants used in the age calculations we refer to Table 2 of *Koppers et al.* [2003a]. Incremental heating plateau ages and isochron ages were calculated as weighted means with  $1/\sigma^2$  as weighting factor [Taylor, 2003] and as YORK2 least squares fits with correlated errors [York, 1969] using the ArArCALC v2.4 software from *Koppers* [2002] that is available from the <http://earthref.org/tools/ararcalc.htm> Web site. In this paper, all errors on the <sup>40</sup>Ar/<sup>39</sup>Ar ages are reported at the 95% confidence level (2σ), unless otherwise indicated.

[8] To determine whether an incremental heating experiment yields meaningful crystallization ages, we adopted the following quality criteria proposed by *Fleck et al.* [1977] and *Pringle* [1993]: (1) high temperature plateaus in the age spectra should include more than three incremental heating steps and at least 50% of the total amount of <sup>39</sup>Ar<sub>K</sub> released, (2) the plateau and isochron ages should be concordant at the 95% confidence level, (3) the <sup>40</sup>Ar/<sup>36</sup>Ar intercepts on the isochron diagrams should be concordant with the atmospheric value of 295.5 at the 95% confidence level, and (4) the mean square of weighted deviations [York, 1969; Roddick, 1978] for both the plateau ages (MSWD = SUMS/N-1) and isochron ages (MSWD = SUMS/

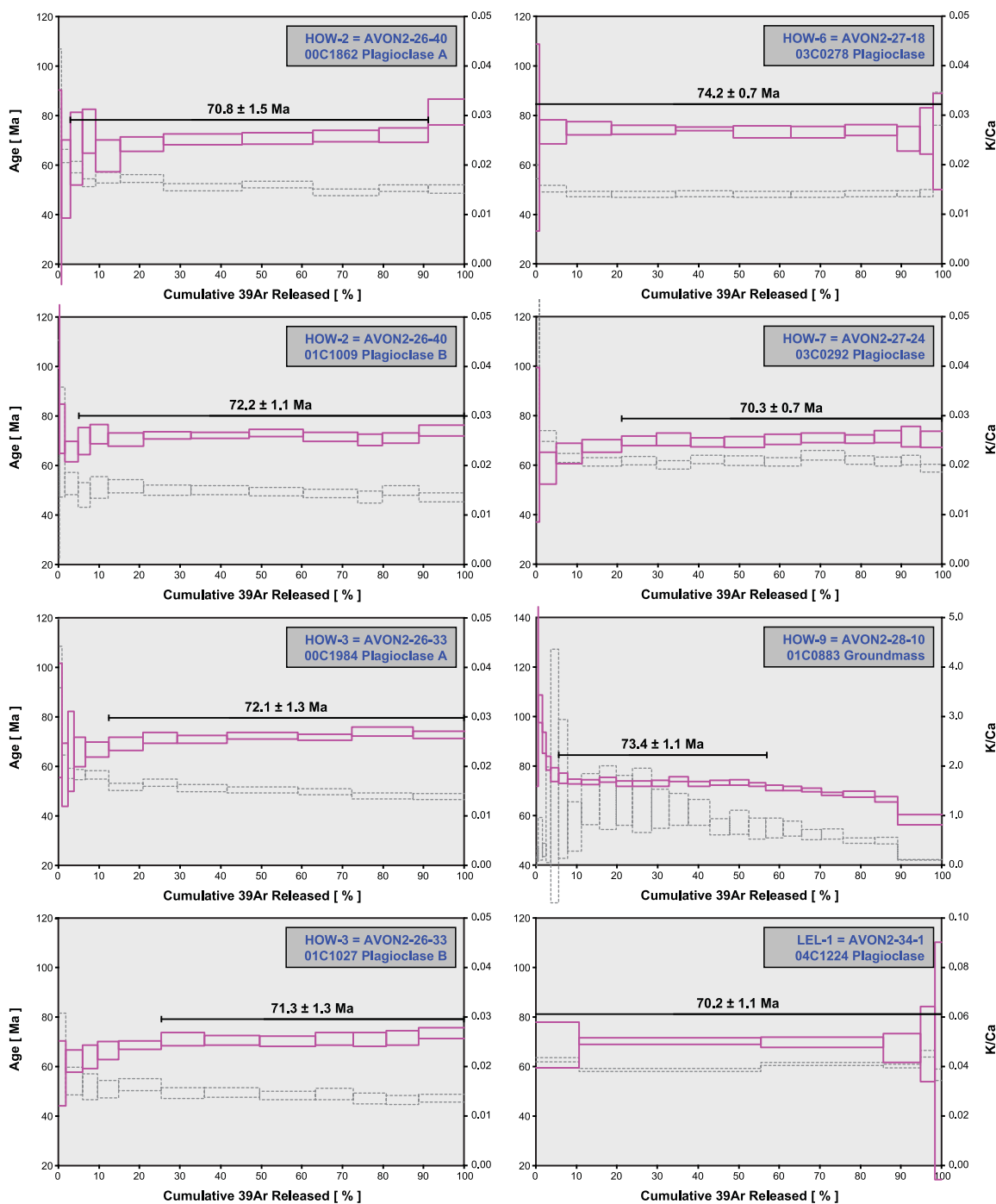


Figure 2. (continued)

N-2) should be sufficiently small if compared to Student's t-test and F-statistic critical values for significance, respectively.

[9] Although these criteria are well suited for the evaluation of <sup>40</sup>Ar/<sup>39</sup>Ar results from unaltered whole-rock samples and mineral separates, they are not always suitable for the evaluation of altered

groundmass separates from submarine basalts [Koppers et al., 2000]. Several reasons can be forwarded to explain this. First of all, because of the intensive acid-leaching of the groundmass samples, the majority of the atmospheric component (from alteration, absorption and trapped argon) is effectively removed from the samples and may result in extremely high radiogenic com-

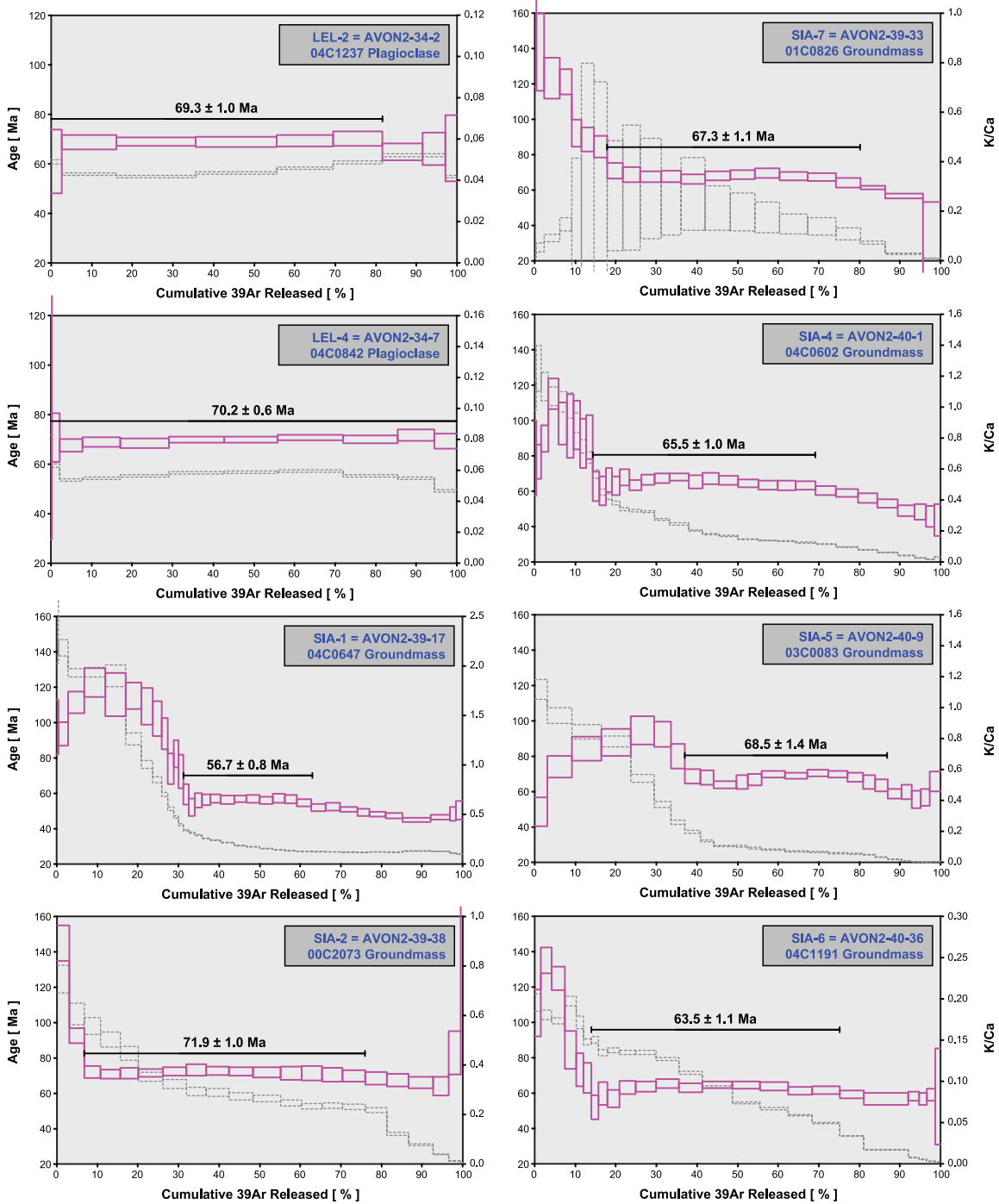


Figure 2. (continued)

ponents for the age plateaus. As a result, the dispersion in the data points is sometimes insufficient to calculate meaningful isochrons owing to a clustering of data points near the radiogenic intercept on the <sup>39</sup>Ar/<sup>40</sup>Ar axis. We consider the data points too radiogenic to calculate meaningful isochrons, if the radiogenic components for all steps included in the age calculations are higher than

95% (Tables 2a and 2b). A second reason why groundmass analyses are harder to evaluate is because of the remaining alteration in the samples, even after intensive acid-leaching. This remaining alteration typically causes a slight sloping of the age plateaus and MSWDs higher than 1. If this is the case, the reported analytical errors are multiplied by the  $\sqrt{\text{MSWD}}$  [York, 1969; Kullerud,

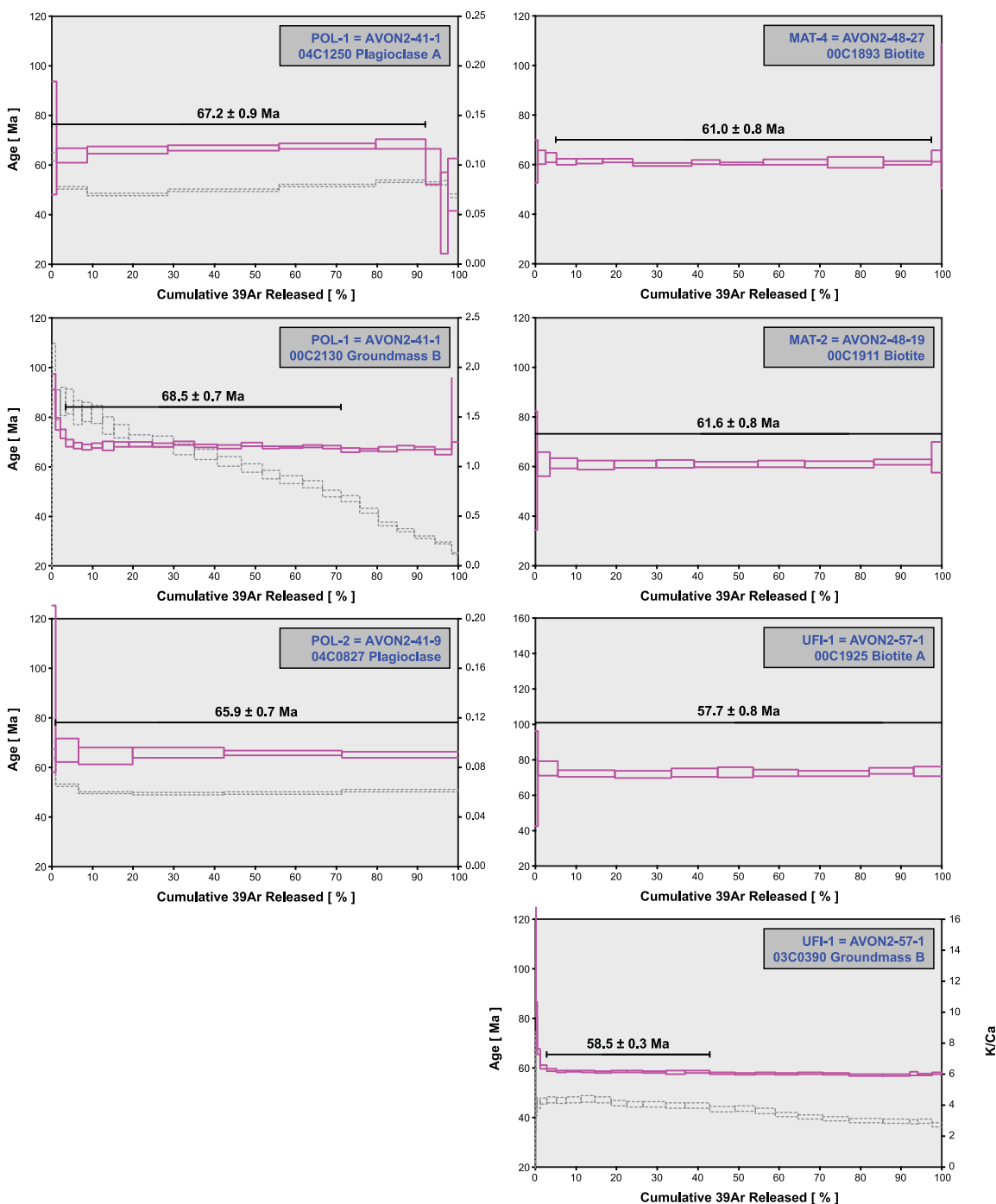
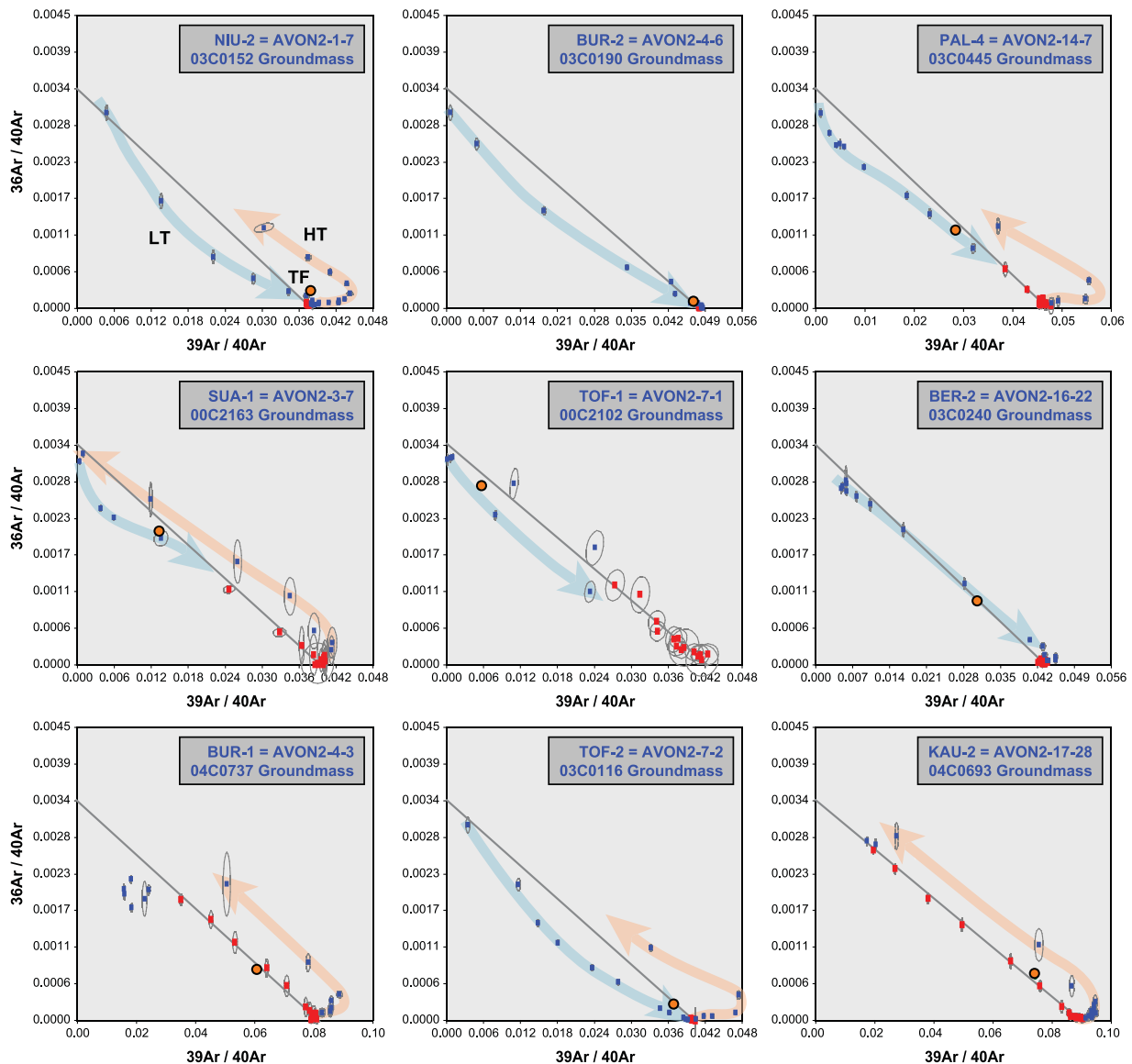


Figure 2. (continued)

1991]. The maximum allowable MSWD is either given by the Student's t-test for plateau ages or the F-statistical analysis for isochron ages, both of which are dependent on the number of data points included in the age calculations. If the MSWD is larger than this value, analytical errors alone cannot explain the scatter about the weighted mean or in the isochron calculation, and ages derived from

these calculations require further justification to be acceptable [Pringle, 1993].

[10] To circumvent bias due to alteration in our groundmass samples and to better evaluate the reproducibility of our <sup>40</sup>Ar/<sup>39</sup>Ar ages, we have performed duplicate analyses if comagmatic phenocrystic phases of plagioclase, hornblende or biotite were available. Whereas some minor differ-



**Figure 3.** Representative set of high-resolution incremental heating <sup>40</sup>Ar/<sup>39</sup>Ar isochron analyses on crystalline groundmass samples for Gilbert Ridge and Tokelau seamount trail basalts. Note that “reference lines” are shown (defined by the 295.5 atmospheric intercept on the <sup>36</sup>Ar/<sup>40</sup>Ar axis and by the plateau age on the <sup>39</sup>Ar/<sup>40</sup>Ar axis) instead of the calculated isochrons. Blue and orange arrows indicate the low-temperature (LT) and high-temperature (HT) incremental heating steps, whereas red squares indicate the steps included in the age calculations. The locations of the total fusion (TF) points are indicated by orange circles. Analytical details are the same as described in Figure 2.

ences are evident between the groundmass and mineral ages, most likely as a result of the remaining alteration, the duplicate analyses yield reproducible ages on the 95% confidence level.

### 3. Geological Setting

[11] The Gilbert Ridge and Tokelau Seamounts are two seamount trails that are located close to one another on the Pacific plate, in between the South Pacific Superswell [McNutt and Judge, 1990] and

the West Pacific Seamount Province (WSP) [Koppers *et al.*, 2003b]. They comprise parallel trends and on the basis of absolute plate motion models [e.g., Duncan and Clague, 1985] would have ages between 30 and 65 Ma, with prominent HEB-type bends that formed around 43 or 47 Ma [Wessel *et al.*, 2003; Kroenke *et al.*, 2004; Sharp and Clague, 2006] depending on the age estimate used for the HEB. Their morphologies were mapped out during a dredging and multibeam cruise on board the R/V *Melville* of the Scripps Institution

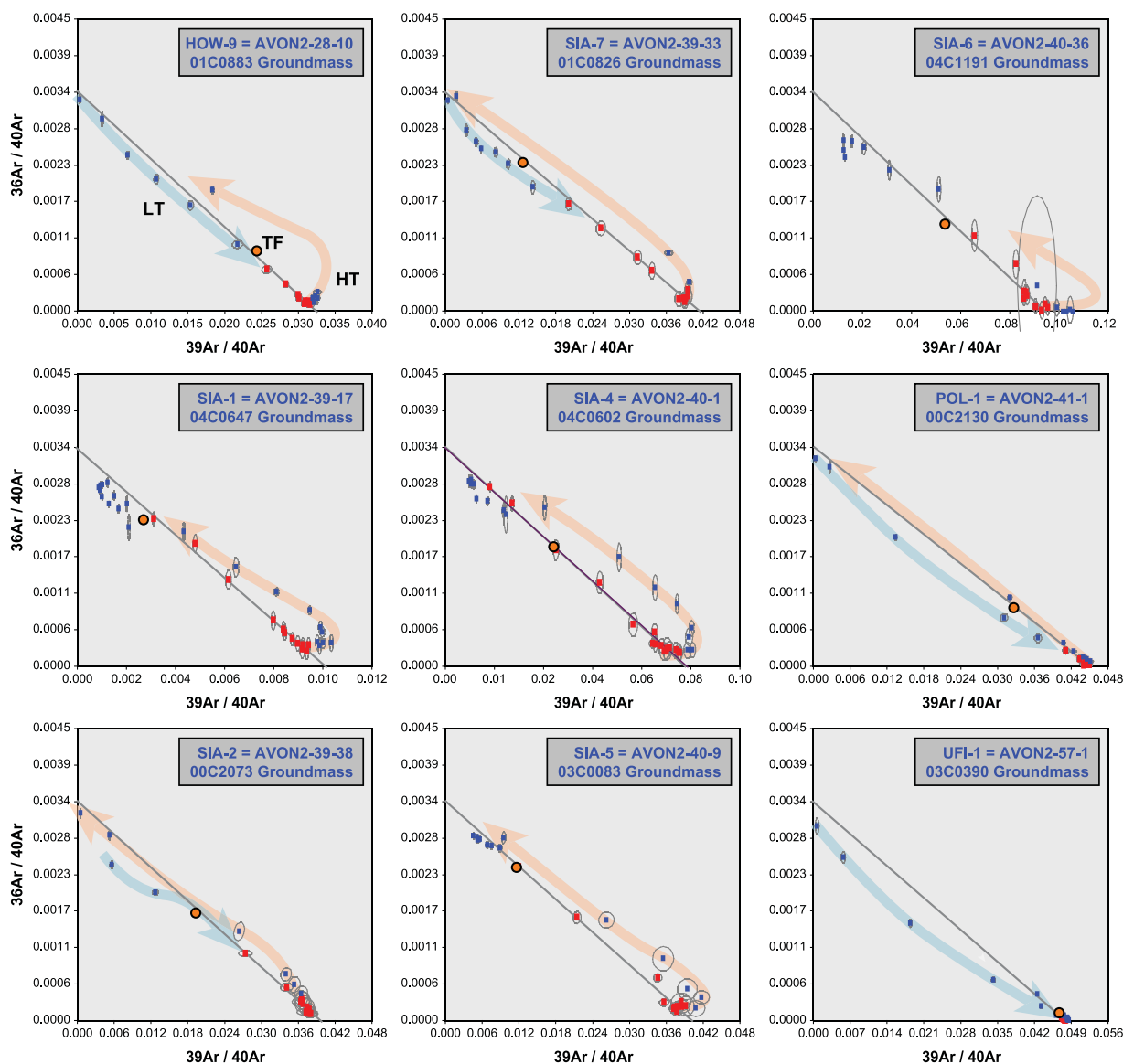


Figure 3. (continued)

of Oceanography in Jan–Feb 1999 (Figure 1). Bathymetric maps for each surveyed seamount are available from the online Seamount Catalog (see Appendix B).

### 3.1. Gilbert Ridge

[12] The Gilbert Ridge is oriented roughly parallel to the Phoenix fracture zone and was formed by sometimes voluminous volcanism (up to  $10^4 \text{ km}^3$  per seamount) on top of predominantly Jurassic age lithosphere. Because of their location in the tropics and their original elevation above sea level, many of these ancient volcanoes are the foundations of coral reefs and atolls. The Gilbert Ridge forms the southern continuation of the Ratak Chain

in the Marshall Islands, with a sharp HEB-type bend around the equator (Figure 1a). Most of these seamounts formed away from oceanic spreading centers, on crust more than 60 Myr old, with the exception of a group of small-volume seamounts that formed on very young oceanic crust to the east of the Phoenix Fracture zone. The Gilbert Ridge also rides on the edge of a region of “anomalously” shallow seafloor (Figure 1) that may have been thermally reactivated as part of the Darwin Rise [Menard, 1964, 1984; McNutt and Menard, 1978; Hillier and Watts, 2005]. More likely this basement has been thickened because of the emplacement of volcanic sills during the formation of the Ontong Java and Manihiki Plateaus around 125 Ma [Tarduno et al., 1991; Castillo et al., 1994;



**Table 1.** Sample Locations in the Gilbert Ridge and Tokelau Seamount Trails

Sample	Seamount Name	Lat	Lon	Depth Range, mbsf
<i>Gilbert Ridge</i>				
AVON2-1-7	Niu	4°37.3'N	172°21.1'E	3,521–3,861
AVON2-3-7	Sua	4°14.8'N	172°23.5'E	2,189–1,936
AVON2-4-3	Burtaritari	2°41.9'N	172°48.2'E	3,564–2,260
AVON2-4-6	Burtaritari	2°41.9'N	172°48.2'E	3,564–2,260
AVON2-5-5	Musina	2°29.3'N	172°51.7'E	3,727–2,285
AVON2-7-1	Tofe Tolu	0°46.8'N	173°16.1'E	3,381–3,289
AVON2-7-2	Tofe Tolu	0°46.8'N	173°16.1'E	3,381–3,289
AVON2-14-7	Palutu	0°55.0'S	175°29.0'E	3,040–2,230
AVON2-16-22	Beru	1°08.5'S	175°43.7'E	3,901–3,280
AVON2-17-28	Kautu	1°20.8'S	175°20.6'E	4,279–3,188
AVON2-18-16	Ava	2°15.6'S	174°52.9'E	3,862–2,621
AVON2-24-16	Sakau	2°18.8'S	177°43.8'E	4,160–3,170
AVON2-24-30	Sakau	2°18.8'S	177°43.8'E	4,160–3,170
AVON2-25-6	Seka	2°28.7'S	179°05.3'E	3,346–2,964
AVON2-25-47	Seka	2°28.7'S	179°05.3'E	3,346–2,964
AVON2-25-48	Seka	2°28.7'S	179°05.3'E	3,346–2,964
<i>Tokelau Seamounts</i>				
AVON2-26-40	Howland	0°50.6'N	176°45.1'W	3,666–2,427
AVON2-26-33	Howland	0°50.6'N	176°45.1'W	3,666–2,427
AVON2-27-18	Howland	0°58.3'N	176°34.3'W	4,756–3,785
AVON2-27-24	Howland	0°58.3'N	176°34.3'W	4,756–3,785
AVON2-28-10	Howland	0°40.2'N	176°32.1'W	4,442–3,370
AVON2-34-1	Lelei	1°04.4'S	176°11.5'W	3,342–2,250
AVON2-34-2	Lelei	1°04.4'S	176°11.5'W	3,342–2,250
AVON2-34-7	Lelei	1°04.4'S	176°11.5'W	3,342–2,250
AVON2-39-17	Siapo	2°36.2'S	175°25.0'W	3,681–2,820
AVON2-39-38	Siapo	2°36.2'S	175°25.0'W	3,681–2,820
AVON2-39-33	Siapo	2°36.2'S	175°25.0'W	3,681–2,820
AVON2-40-1	Siapo	2°34.0'S	175°25.6'W	3,582–2,379
AVON2-40-9	Siapo	2°34.0'S	175°25.6'W	3,582–2,379
AVON2-40-36	Siapo	2°34.0'S	175°25.6'W	3,582–2,379
AVON2-41-1	Polo	2°46.9'S	175°09.0'W	4,045–3,461
AVON2-41-9	Polo	2°46.9'S	175°09.0'W	4,045–3,461
AVON2-48-19	Matai	6°41.9'S	173°28.0'W	3,227–2,001
AVON2-48-27	Matai	6°41.9'S	173°28.0'W	3,227–2,001
AVON2-57-1	Ufiata	8°16.3'S	172°52.7'W	3,152–2,056

Larson, 1997; Mochizuki *et al.*, 2005; Taylor, 2006]. As a result, the intrusion of Ontong Java Plateau basalts in the Nauru Basin may have weakened or preconditioned the Pacific lithosphere for later seamount emplacements. Multichannel seismic reflection and refraction data from the Nauru Basin [Mochizuki *et al.*, 2005] shows the presence of a 2,200–5,500 m thick volcanic complex (of sills in between the sediment layers) that explains the anomalous shallow seafloor underneath the Gilbert Ridge.

### 3.2. Tokelau Seamounts

[13] The Tokelau seamount chain is less voluminous than the Gilbert Ridge with two HEB-type bends around 9°S and 3°S (Figure 1). Most of the Tokelau Seamounts sit on oceanic crust that was formed during the Cretaceous quite zone or

M1 time. This crust apparently was not influenced by the formation of the Darwin Rise, Ontong Java Plateau or any large offset transform faults, but hosts the Nova Canton Trough that rifted (and quickly became inactive again) between 121–118 Ma [Larson, 1997; Larson and Erba, 1999] and the western extension of the Manihiki plateau that intervenes with the southern end of this seamount trail. Both bends are also associated with a cessation of volcanism, where the upper trail terminates in the middle of the Nova Canton Trough and the lower trail terminates on a northwestern extension of the Manihiki plateau.

### 4. Results

[14] Our dredging targeted deep volcanic features at the base of the Gilbert Ridge and Tokelau

**Table 2a.** Incremental Heating <sup>40</sup>Ar/<sup>39</sup>Ar Analyses on the Gilbert Ridge Seamount Trail<sup>a</sup>

Sample	Lab Code	Experiment	Sample Type	Duplicate Number	Age Spectrum			Total Fusion		Inverse Isochron Analyses <sup>b</sup>			
					Age ± 2σ, Ma	<sup>39</sup> Ar, %	K/Ca	MSWD	n	Age ± 2σ, Ma	<sup>40</sup> Ar/ <sup>36</sup> Ar Intercept	MSWD	
AVON2-1-7	NIU-2	03C0152	groundmass		70.8 ± 0.5	26	0.297	1.0	7				
AVON2-3-7	SUA-1	00C2163	groundmass		69.4 ± 1.3	58	0.083	1.2	12	81.1 ± 1.6	67.9 ± 1.7	346.1 ± 60.6	0.6
AVON2-4-3	BUR-1	04C0737*	groundmass		70.8 ± 0.6	66	0.351	1.8	17	73.2 ± 0.5	70.7 ± 0.6	298.5 ± 17.1	1.9
AVON2-4-6	BUR-2	03C0190*	groundmass		72.3 ± 0.5	43	0.189	2.1	9	74.9 ± 0.5			
AVON2-5-5	MUS-2	00C1878*	hornblende	A	68.9 ± 0.8	91	0.080	0.6	6	69.0 ± 0.8			
		01C0991*	hornblende	B	69.4 ± 1.1	100	0.073	1.5	8	71.0 ± 1.0	70.5 ± 1.0	309.9 ± 12.3	0.8
AVON2-7-1	TOF-1	03C0330*	plagioclase	A	67.1 ± 0.5	97	0.017	0.9	8	67.3 ± 0.6	67.0 ± 0.6	312.2 ± 43.1	0.9
		00C2102*	groundmass	B	65.5 ± 1.2	83	0.022	0.8	14	91.6 ± 7.9	65.2 ± 1.7	310.7 ± 57.1	0.8
AVON2-7-2	TOF-2	03C0116	groundmass		70.3 ± 0.4	44	0.264	1.2	9	70.9 ± 0.4			
AVON2-14-7	PAL-4	03C0445*	groundmass		63.7 ± 0.5	63	0.101	2.3	14	67.9 ± 0.5	63.4 ± 0.9	331.6 ± 88.7	2.3
AVON2-16-22	BER-2	03C0240*	groundmass		65.7 ± 0.7	51	0.136	5.0	11	66.2 ± 0.5			
AVON2-17-28	KAU-2	04C1168*	hornblende	A	63.9 ± 1.3	100	0.060	0.3	8	64.2 ± 1.7	63.7 ± 1.4	307.8 ± 35.5	0.2
		04C0693*	groundmass	B	65.5 ± 0.5	54	0.460	2.0	17	63.1 ± 0.4	65.4 ± 0.5	301.2 ± 6.4	1.8
AVON2-18-16	AVA-1	04C0857	plagioclase		77.9 ± 0.5	100	0.074	1.9	15	78.1 ± 0.4	77.9 ± 1.4	318.4 ± 19.8	0.4
AVON2-24-16	SAK-1	03C0343	plagioclase		74.7 ± 0.4	100	0.112	2.0	14	74.7 ± 0.4	74.8 ± 0.7	282.6 ± 47.3	2.1
AVON2-24-30	SAK-2	03C0362	plagioclase		75.1 ± 0.3	80	0.136	0.4	8	75.0 ± 0.3	75.0 ± 1.3	305.7 ± 102	0.5
AVON2-25-6	SEK-3	04C0796	plagioclase		115.3 ± 1.0	98	0.034	0.5	7	114.9 ± 1.2	115.3 ± 3.6	337.4 ± 115	0.7
AVON2-25-47	SEK-6	03C0311	plagioclase	A	110.7 ± 0.7	73	0.020	0.7	11	112.2 ± 0.6	110.6 ± 0.7	297.5 ± 10.1	0.7
		04C0878	plagioclase	B	116.4 ± 0.8	100	0.015	0.8	12	116.4 ± 0.9	116.4 ± 0.9	314.8 ± 117	0.8
AVON2-25-48	SEK-7	04C0808	plagioclase		113.5 ± 0.8	97	0.016	1.1	10	114.0 ± 0.9			

<sup>a</sup> K/Ca values are calculated as weighted means for the age spectra or using recombined totals of <sup>39</sup>Ar<sub>K</sub> and <sup>37</sup>Ar<sub>Ca</sub> for the total fusions. MSWD values for the age plateaus and inverse isochrons are calculated using N-1 and N-2 degrees of freedom, respectively. All samples from this study where monitored against FCT-3 biotite (28.04 ± 0.18 Ma) as calibrated by Renne *et al.* [1998]. Reported errors on the <sup>40</sup>Ar/<sup>39</sup>Ar ages are on the 95% confidence level including 0.3–0.4% standard deviation in the J-value. All input parameters to the calculations are published in Table 2 of Koppers *et al.* [2003a]. Age data previously published by Koppers and Staudigel [2005] are denoted by an asterisk.

<sup>b</sup> In some cases the inverse isochron could not be calculated because the samples are too radiogenic.

**Table 2b.** Incremental Heating <sup>40</sup>Ar/<sup>39</sup>Ar Analyses on the Tokelau Seamount Trail<sup>a</sup>

Sample	Lab Code	Experiment	Sample Type	Duplicate Number	Age Spectrum			Total Fusion			Inverse Isochron Analyses <sup>b</sup>		
					Age ± 2σ, Ma	<sup>39</sup> Ar, %	K/Ca	MSWD	n	Age ± 2σ, Ma	Age ± 2σ, Ma	<sup>40</sup> Ar/ <sup>36</sup> Ar Intercept	MSWD
AVON2-26-40	HOW-2	00C1862	plagioclase	A	70.8 ± 1.5	88	0.016	1.4	8	70.9 ± 1.5	71.6 ± 2.4	327.0 ± 105	1.4
		01C1009	plagioclase	B	72.2 ± 1.1	95	0.015	1.3	10	72.2 ± 1.1			
AVON2-26-33	HOW-3	00C1984	plagioclase	A	72.1 ± 1.3	88	0.015	2.2	7	71.3 ± 1.2			
		01C1027	plagioclase	B	71.3 ± 1.3	75	0.014	1.0	7	69.9 ± 1.2			
AVON2-27-18	HOW-6	03C0278	plagioclase		74.2 ± 0.7	100	0.015	0.5	11	73.6 ± 1.0	73.8 ± 1.0	286.4 ± 34.2	0.3
AVON2-27-24	HOW-7	03C0292	plagioclase		70.3 ± 0.7	79	0.021	0.5	10	69.3 ± 0.8	67.8 ± 4.3	316.7 ± 35.8	0.4
AVON2-28-10	HOW-9	01C0883	groundmass		73.4 ± 1.1	51	0.743	1.3	12	71.1 ± 1.1	73.0 ± 1.3	328.0 ± 44.7	1.8
AVON2-34-1	LEL-1	04C1224*	plagioclase		70.2 ± 1.1	100	0.041	0.2	6	69.7 ± 1.7			
AVON2-34-2	LEL-2	04C1237*	plagioclase		69.3 ± 1.0	82	0.045	0.5	6	68.5 ± 1.1	69.7 ± 1.1	263.0 ± 56.9	0.3
AVON2-34-7	LEL-4	04C0842*	plagioclase		70.2 ± 0.6	100	0.056	1.3	11	70.1 ± 0.6			
AVON2-39-17	SIA-1	04C0647	groundmass		56.7 ± 0.8	32	0.174	0.7	12	69.6 ± 1.1	56.6 ± 0.9	296.6 ± 12.7	0.8
AVON2-39-38	SIA-2	00C2073	groundmass		71.9 ± 1.0	69	0.275	0.4	13	75.6 ± 1.3	72.1 ± 1.2	287.9 ± 33.4	0.4
AVON2-39-33	SIA-7	01C0826*	groundmass		67.3 ± 1.1	62	0.143	1.6	11	70.7 ± 1.6	66.7 ± 1.4	311.2 ± 22.3	1.5
AVON2-40-1	SIA-4	04C0602*	groundmass		65.5 ± 1.0	55	0.172	1.8	16	66.2 ± 0.9	65.6 ± 1.1	292.4 ± 9.8	1.8
AVON2-40-9	SIA-5	03C0083*	groundmass		68.5 ± 1.4	47	0.073	3.7	11	72.3 ± 1.2	68.6 ± 1.6	294.4 ± 15.2	4.0
AVON2-40-36	SIA-6	04C1191*	groundmass		63.5 ± 1.1	60	0.073	2.1	11	67.3 ± 0.9	63.6 ± 1.4	286.7 ± 83.6	2.3
AVON2-41-1	POL-1	04C1250*	plagioclase	A	67.2 ± 0.9	92	0.077	2.1	6	66.0 ± 0.8	66.5 ± 2.1	330.1 ± 60.0	0.8
		00C2130	groundmass	B	68.5 ± 0.7	68	1.020	2.2	16	69.4 ± 0.9	68.3 ± 0.8	356.4 ± 117	2.3
AVON2-41-9	POL-2	04C0827*	plagioclase		65.9 ± 0.7	99	0.061	0.4	5	66.2 ± 0.9	61.5 ± 0.9	300.1 ± 80.4	0.3
AVON2-48-19	MAT-2	00C1911*	biotite		61.6 ± 0.8	100	3.825	0.3	11	61.6 ± 0.8			
AVON2-48-27	MAT-4	00C1893*	biotite		61.0 ± 0.8	92	5.182	1.8	9	61.3 ± 0.8			
AVON2-57-1	UFI-1	00C1925*	biotite	A	57.7 ± 0.8	100	2.295	0.6	10	57.7 ± 0.8	57.6 ± 0.9	325.3 ± 98.2	0.6
		03C0390*	groundmass	B	58.5 ± 0.3	38	4.198	0.5	9	58.3 ± 0.3			

<sup>a</sup>See Table 2a footnote.

<sup>b</sup>In some cases the inverse isochron could not be calculated because the samples are too radiogenic.



Seamounts, recovering mostly aphyric or olivine- and clinopyroxene-bearing basalts, with more evolved rock types being absent in all of our dredges. Although this rock suite reflects the depleted and early stage of shield volcanism in the construction of these seamounts, it also offered challenges for  $^{40}\text{Ar}/^{39}\text{Ar}$  dating due to low potassium abundances and severe seawater alteration. We could overcome these problems, however, through the dating of phenocrystic plagioclase, hornblende and biotite phases, or in case these were unavailable, acid-leached groundmass separates. In this section, we interpret the  $^{40}\text{Ar}/^{39}\text{Ar}$  age spectra (Figures 2 and 3) and assess the quality of the groundmass incremental heating experiments. We also interpret our new age results for the Gilbert Ridge and Tokelau seamount trails in the context of their observed (nonlinear) age systematics.

#### 4.1. $^{40}\text{Ar}/^{39}\text{Ar}$ Geochronology

[15] Twenty-five mineral separates of plagioclase, hornblende or biotite have been dated using the  $^{40}\text{Ar}/^{39}\text{Ar}$  incremental heating technique. The age spectra of these analyses (Figure 2) have generally well-developed plateaus, including more than 73% of the released  $^{39}\text{Ar}_K$  and 6 to 15 individual heating steps. Their associated MSWDs range from 0.2 to 2.2 and are all lower than the critical values for the Student's t-test and F-statistical analysis, indicating scatter from analytical uncertainties only. The  $^{40}\text{Ar}/^{36}\text{Ar}$  intercepts from the inverse isochron calculations are within error of the atmospheric value (295.5) and whenever repeated analyses were performed from different grain-size fractions or acid-leaching procedures, the reproducibility is very good, with the  $^{40}\text{Ar}/^{39}\text{Ar}$  ages being indistinguishable at the  $2\sigma$  confidence level. We thus conclude that the  $^{40}\text{Ar}/^{39}\text{Ar}$  ages on the mineral separates can be reliably used to infer crystallization ages for the Gilbert Ridge and Tokelau Seamounts basalts.

[16] If no good-quality phenocryst phases were available for  $^{40}\text{Ar}/^{39}\text{Ar}$  dating, we prepared acid-leached holocrystalline groundmass samples and performed incremental heating experiments comprising between 21 and 35 individual heating steps (Figure 2). In total we carried out eighteen experiments, giving age plateaus typically ranging between 40 and 80% of the released  $^{39}\text{Ar}_K$  and including between 7 and 17 individual heating steps. The quality and usefulness of groundmass  $^{40}\text{Ar}/^{39}\text{Ar}$  age dating have been described in detail

before [Koppers *et al.*, 2000, 2003a, 2003b, 2004], but nonetheless we highlight a few key observations that are helpful in the interpretation of these kind of  $^{40}\text{Ar}/^{39}\text{Ar}$  analyses. First of all, the argon age spectra systematically exhibit deviations with higher ages for the low-temperature (LT) increments and lower ages for the high-temperature (HT) increments (Figure 2). The apparently higher ages are well understood in light of the very fine-grained alteration in the basaltic groundmass that may remain, even after the intense acid-leaching procedures carried out here, and is very sensitive to  $^{39}\text{Ar}_K$  recoil loss during the sample irradiation. This alteration signature is also obvious from the K/Ca ratios that are higher for the LT increments and reflect a significant contribution of potassium-rich alteration minerals in the argon signal. On the other hand, recoil loss of  $^{37}\text{Ar}_{Ca}$  most likely causes the apparently lower ages for the HT increments, which are characterized by a preferential degassing of the Ca-rich plagioclase and clinopyroxene minerals in the groundmasses, as reflected in the low K/Ca ratios (Figure 2). These characteristics are also evident from the inverse isochron diagrams (Figure 3) where the LT increments typically follow a concave curve (light blue arrows) between the  $^{40}\text{Ar}/^{36}\text{Ar}$  intercept and the isochron itself, and the HT increments follow a convex curve (orange arrows) that first moves toward higher  $^{39}\text{Ar}/^{40}\text{Ar}$  ratios and then back to the atmospheric intercept. The age plateaus, nevertheless, have high radiogenic  $^{40}\text{Ar}$  components and depict linear trends in the inverse isochron diagrams (red squares) that run parallel to the “reference line” between the plateau age on the  $^{39}\text{Ar}/^{40}\text{Ar}$  axis and the 295.5 atmospheric intercept on the  $^{36}\text{Ar}/^{40}\text{Ar}$  axis (Figure 3). These distinct bimodal mixing arrays indicate that the age plateaus are not significantly affected by either alteration or recoil. However, this does not mean that the alteration and recoil effects have been completely eliminated from the groundmass samples by the intense acid-leaching. Most groundmass age plateaus still reveal subtle increasing and decreasing trends within the  $2\sigma$  plateau age envelop that can be attributed to the remaining effects of alteration and recoil, partially explaining the larger range in observed MSWDs from 0.4 to 5.0 (Tables 2a and 2b) as compared with the mineral data.

[17] Despite the complexity of their age spectra and the lingering effects of seawater alteration, the groundmass ages have been shown to be compatible with  $^{40}\text{Ar}/^{39}\text{Ar}$  ages of comagmatic plagioclase and hornblende mineral phases [Koppers *et al.*,

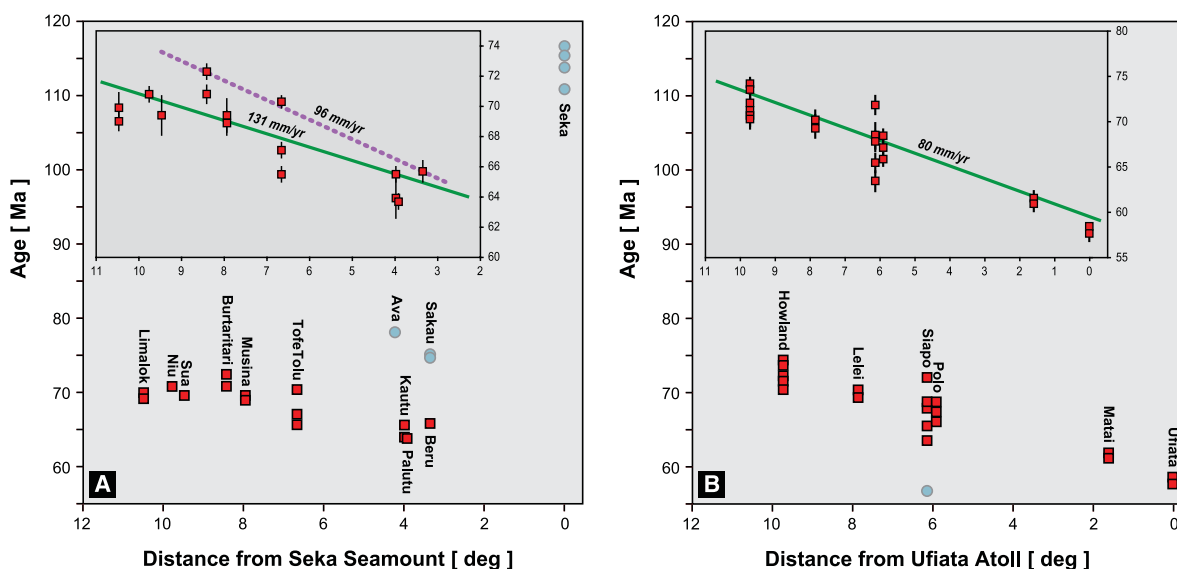


**Figure 4.** Age versus distance plots for (a) the Gilbert Ridge and (b) the Tokelau Seamounts. Even though clear age decreasing trends exist from the north to the south in both seamount trails, the resulting linear age progressions are too fast if compared to the 62 and 74 mm/yr as derived from the most recent plate motion models. In addition, a considerable difference in the measured plate velocities exists between the Gilbert Ridge (96–131 mm/yr) and Tokelau seamount trail (80 mm/yr) that is difficult to reconcile with the “fixed” hot spot hypothesis, because their close proximity would demand similar azimuths and plate velocities.

2000]. In this study, we analyzed four more groundmass/mineral pairs to verify the reproducibility and quality of single groundmass analyses. The results are very promising, with each age pair being concordant on the  $2\sigma$  confidence level: (1)  $67.1 \pm 0.5$  Ma (plag) and  $65.5 \pm 1.2$  Ma (grndm) for sample TOF-1; (2)  $63.9 \pm 1.3$  Ma (hbl) and  $65.5 \pm 0.5$  Ma (grndm) for sample KAU-2; (3)  $67.2 \pm 0.9$  Ma (plag) and  $68.5 \pm 0.7$  Ma (grndm) for sample POL-1; (4)  $57.7 \pm 0.8$  Ma (bio) and  $58.5 \pm 0.3$  Ma (grndm) for sample UFI-1. We conclude therefore that the groundmass <sup>40</sup>Ar/<sup>39</sup>Ar age dating technique can be used reliably to estimate the crystallization age of seamount basalt samples, if no good-quality mineral phases are available for dating.

#### 4.2. Observed Seamount Trail Age Systematics

[18] Along the aligned volcanic edifices of the Gilbert Ridge no apparent age progression in any direction is demonstrated by the existing data. However, if we force a regression through this highly nonlinear data set, it would indicate an “ultra-fast” plate velocity of  $\sim 131$  mm/yr and a younging toward the southern end of the Gilbert Ridge (Figure 4a). While such high plate velocities are possible, they are inconsistent with absolute

plate motion models that predict local plate velocities between 62 and 74 mm/yr [Duncan and Clague, 1985; Lonsdale, 1988; Wessel and Kroenke, 1997; Koppers et al., 2001] and the significantly lower plate velocity of the neighboring Tokelau seamount trail (see below). Such reasoning may be regarded circular, because all above plate motion models include Gilbert Ridge seamount locations in their inversions, yet none include any modern age data from this region, making this comparison valid and illustrative.

[19] Besides the unexpectedly high apparent plate velocity of 131 mm/yr, the Gilbert Ridge also includes at least three seamounts that are anomalously older. The very small Sakau and Ava seamounts are  $75.0 \pm 0.2$  Ma ( $n = 2$ ) and  $77.9 \pm 0.5$  Ma (Figure 1) and are located toward the southern extension of this seamount trail. Seka seamount is about  $115 \pm 0.5$  Ma ( $n = 3$ ) and lies to the east of the Phoenix fracture zone, where the oceanic crust is only a few million years older than Seka seamount itself. This latter seamount therefore formed in a plate tectonic setting close to an ancient mid-oceanic ridge system [Batiza, 1982; Batiza and Vanko, 1983]. Sakau and Ava, on the other hand, were formed on ocean floor that was about 50–55 Myr old and most likely would reflect another source of intraplate volcanism than what formed the majority of seamounts in the Gilbert

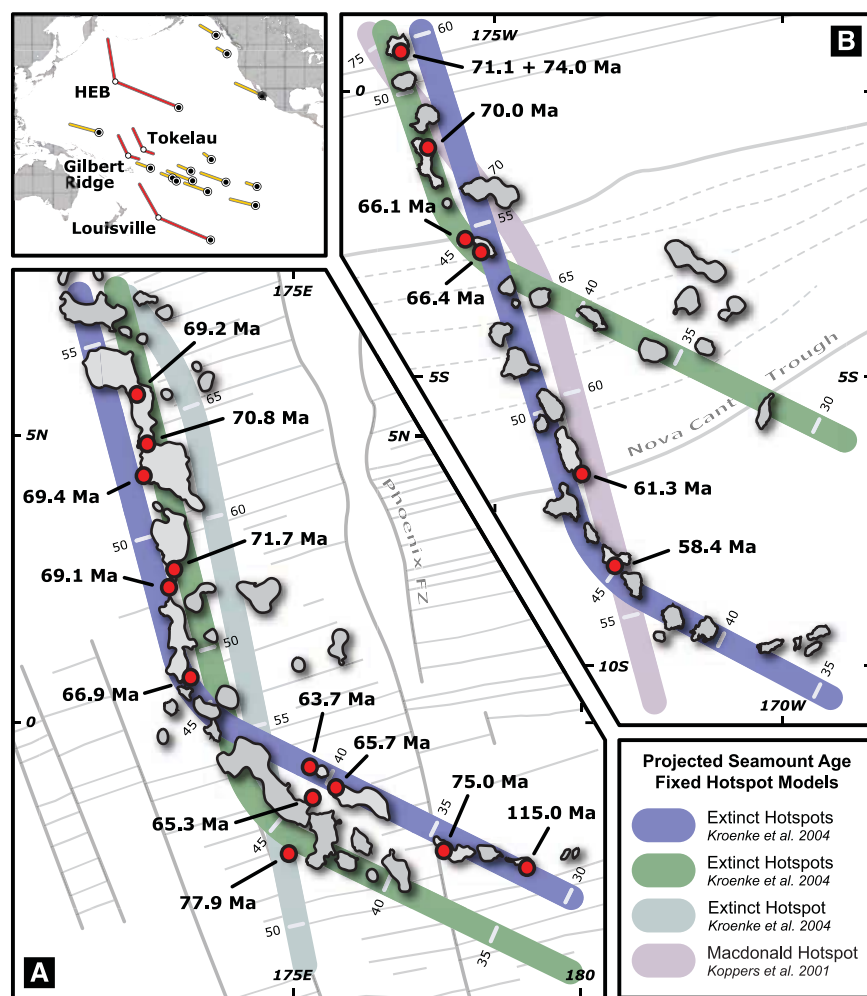


**Figure 5.** Comparing average seamount ages based on <sup>40</sup>Ar/<sup>39</sup>Ar analyses with respect to the predicted plate motion between 30 and 80 Ma as based on the most recent models from Wessel and Kroenke [Wessel et al., 2003; Kroenke et al., 2004] and Koppers et al. [2001] for Macdonald hot spot. All ages are in Ma and have been calculated as weighted means from the ages listed in Table 1. The 69.2 Ma age for Limalok guyot was previously given by Koppers et al. [2000] but has been recalibrated here to reflect the 28.04 Ma FCT-3 age standard. Map modified after Koppers and Staudigel [2005].

Ridge. However, the most surprising finding in the Gilbert Ridge age systematics is the complete mismatch of the measured <sup>40</sup>Ar/<sup>39</sup>Ar ages with the predicted ages (up to 20 Myr) from the absolute plate motion models (Figure 5a). This observation forms the core of our discussion in this paper because it has major implications for our understanding of intraplate volcanism.

[20] The Tokelau seamount trail has a more linear age progression that would translate into a local plate velocity of  $80 \pm 7$  mm/yr (Figure 4b). This is much closer to the 62 to 74 mm/yr estimates from the latest absolute plate motion models, but the measured ages show a similar mismatch with the model ages (Figure 5b) as shown for the Gilbert

Ridge seamounts. In addition, the calculated age progression assumes that only one hot spot formed the entire Tokelau seamount trail, ignoring the sharp bend around 3°S that runs through the center of the Nova Canton Trough (Figure 1b). Unfortunately, not enough age determinations are available to calculate two separate age progressions, but it is interesting to note that by assuming a hot spot origin around the volcanically active Macdonald seamount at the eastern end of the Austral Islands, we would be able to fit the ages measured in the Tokelau seamount trail (Figure 5b) and its geochemical signature [Konter et al., 2004]. However, with this model, we would be unable to explain the observed sharp morphological bends. As it turns



out, this fit is rather model dependent, as we will further discuss in the remainder of this paper.

## 5. Discussion

[21] Both the Gilbert Ridge and Tokelau seamount trails show age systematics that are nonlinear and inconsistent with current absolute plate motion models [Duncan and Clague, 1985; Lonsdale, 1988; Wessel and Kroenke, 1997; Koppers *et al.*, 2001]. It is obvious from our age determinations that plate motion alone, with respect to a fixed reference frame of narrow plumes in the deep mantle, cannot explain the apparent velocities as derived from these age systematics and the asynchronous timing of the HEB-type bends. Either these hot spots have moved significantly with respect to each other or other nonplume processes have contributed to the formation of these seamount trails. In this section, we will first discuss what the fixed hot spot hypothesis would predict for the Gilbert and Tokelau seamount trails and which assumptions are violated by our new age determinations. In the remainder of this section, we will discuss three alternative models that might explain the observed age systematics by the possibility of (1) motion between short-lived hot spots, (2) plate extension due to local changes in plate stress, or (3) multiple intersecting or overlapping hot spot trails.

### 5.1. Fixed Hot Spot Hypothesis

[22] Our geochronological data show that the 47 Ma HEB does not occur in the Gilbert Ridge and Tokelau seamount trails, and conversely, that no consistent morphological evidence exists for 57 and 67 Ma HEB-type bends in the Hawaii-Emperor and Louisville seamount trails. In addition, the Gilbert Ridge shows a highly nonlinear age progression at best, evidence for multiple phases of intraplate volcanism around 115, 74–77 and 67 Ma, and an apparent plate velocity of  $\sim 131$  mm/yr that is very different from the  $\sim 87$  mm/yr velocity calculated for the neighboring Tokelau seamount trail. These observations create a serious dilemma for the fixed hot spot hypothesis, because they violate two assumptions central to this hypothesis: (1) that changes in absolute plate motion are recorded simultaneously in colinear seamount trails, resulting in identical morphological changes, and (2) that hot spots produce corresponding linear age progressions in colinear seamount trails, reflecting the (constant) angular velocity of a rotating rigid tectonic plate over a given period of geological time. Even though

the fixed hot spot hypothesis may allow for the presence of younger volcanism, owing to the long-lived evolution of single volcanoes up to several million of years, it is difficult to explain the presence of older ages in colinear seamount trails, as we observed in our study of the Gilbert Ridge and Tokelau Seamounts.

[23] The utility of the hot spot model for the origin of the Gilbert Ridge and Tokelau seamounts can also be explored by “backtracking” individual seamounts on the basis of their age and particular plate motion models (Figures 6a–6d). It is important to state here that these reconstructions assume the presence of a “fixed” reference frame of hot spots in the Pacific and thus reflect past plate motions only. Also we assume that these hot spots have mantle plumes that are narrow and do not exceed 300 km in diameter. A reasonable fit to Macdonald hot spot can be achieved for the Tokelau Seamounts (Figures 6a and 6d) using the absolute plate motion model of Koppers *et al.* [2001] and Wessel *et al.* [2006] to which we will refer as KMMS01 and WHK06 hereafter. However, the reconstructed seamounts do not cluster and some plot up to 350 km away from the Macdonald hot spot position. The fit deteriorates when we apply the Raymond *et al.* [2000] and the Wessel and Kroenke [1997] models, labeled R20 and WK97, with distances from the reconstructed seamount positions to Macdonald hot spot ranging from 300 to 600 km (Figures 6b and 6c).

[24] The fit of the Gilbert Ridge seamounts to the Rurutu and Mangaia hot spots is even poorer, despite a similar geochemical signature with high <sup>206</sup>Pb/<sup>204</sup>Pb ratios [Konter *et al.*, 2004] that resembles the unique HIMU mantle end-member [Zindler and Hart, 1986]. The reconstructions of Limalok Guyot and seamounts of the Cretaceous Ratak and South Wake seamount trails are very interesting in this context. Limalok guyot was drilled during ODP Leg 144 and resulted in two high-quality <sup>40</sup>Ar/<sup>39</sup>Ar ages of 69.2 Ma [Koppers *et al.*, 2000]. It is part of the Gilbert Ridge seamount trail where it continues into the Ratak Chain to the north, but as can be seen from our reconstructions, its backtracked location is highly uncorrelated and plots 300 to 450 km to the north of the other Gilbert Ridge seamounts (Figure 6). One may argue that its non-HIMU signature [Koppers *et al.*, 2003b] demonstrates that this guyot was formed by another hot spot, yet its high-volume volcanic edifice makes Limalok morphologically identical to the other seamounts in the Gilbert Ridge. The majority of seamounts in the

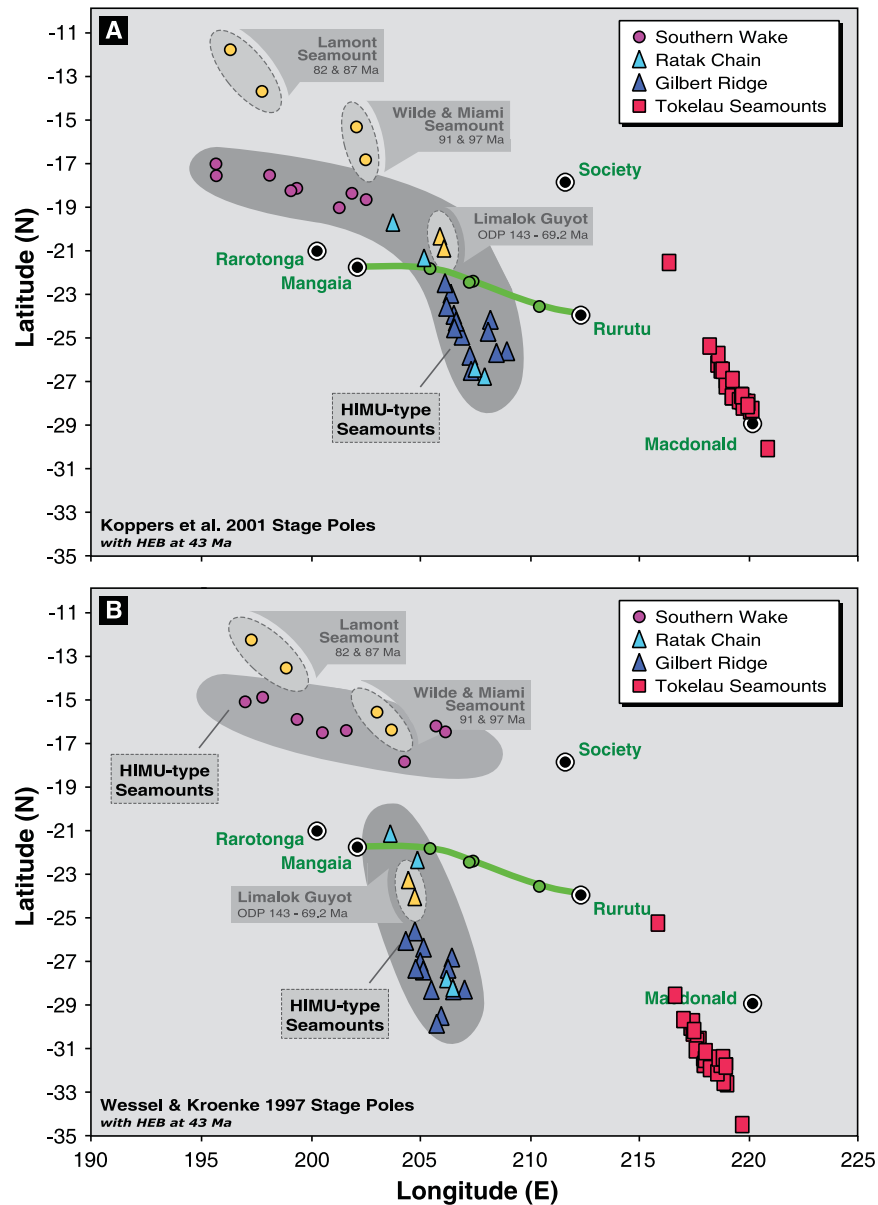


**Figure 6.** Backtrack analyses of the Southern Wake, Ratak, Gilbert Ridge, and Tokelau seamount trails and comparison to the HIMU-type seamounts of the Cook-Austral and Macdonald hot spots in the South Pacific. We show the results from three different stage pole models by (a) *Koppers et al.* [2001], (b) *Wessel and Kroenke* [1997], (c) *Raymond et al.* [2000], and (d) *Wessel et al.* [2006] that all assume an age of 43 Ma for the Hawaii-Emperor Bend (HEB) except in the latter model. However, a systematic ~300 km offset to the northeast will result if we accept an age for the HEB equal to 47 Ma [Sharp and Clague, 2006], which diminishes the fit to the Cook-Austral and Macdonald hot spots significantly. Note that the Southern Wake seamount trail also contains seamounts (yellow circles) that are not HIMU-type and that the active hot spots of the South Pacific region (filled black circles) and HIMU-type seamounts of the Mangaia-Rurutu line (green circles) are shown for reference.

Southern Wake and Ratak seamount trails form another group of (older) seamounts that carry the same HIMU signature [*Koppers et al.*, 2003b] and could potentially relate to the Cook-Austral Islands and the Gilbert Ridge. However, our backtrack reconstructions show that these seamounts plot

even farther to the north of the Gilbert Ridge and Cook-Austral Islands (Figure 6). Although the latter observation might be the result of our poor knowledge of Pacific plate motions prior to 80 Ma, it is evident that different plate motion models substantially influence the results of the seamount

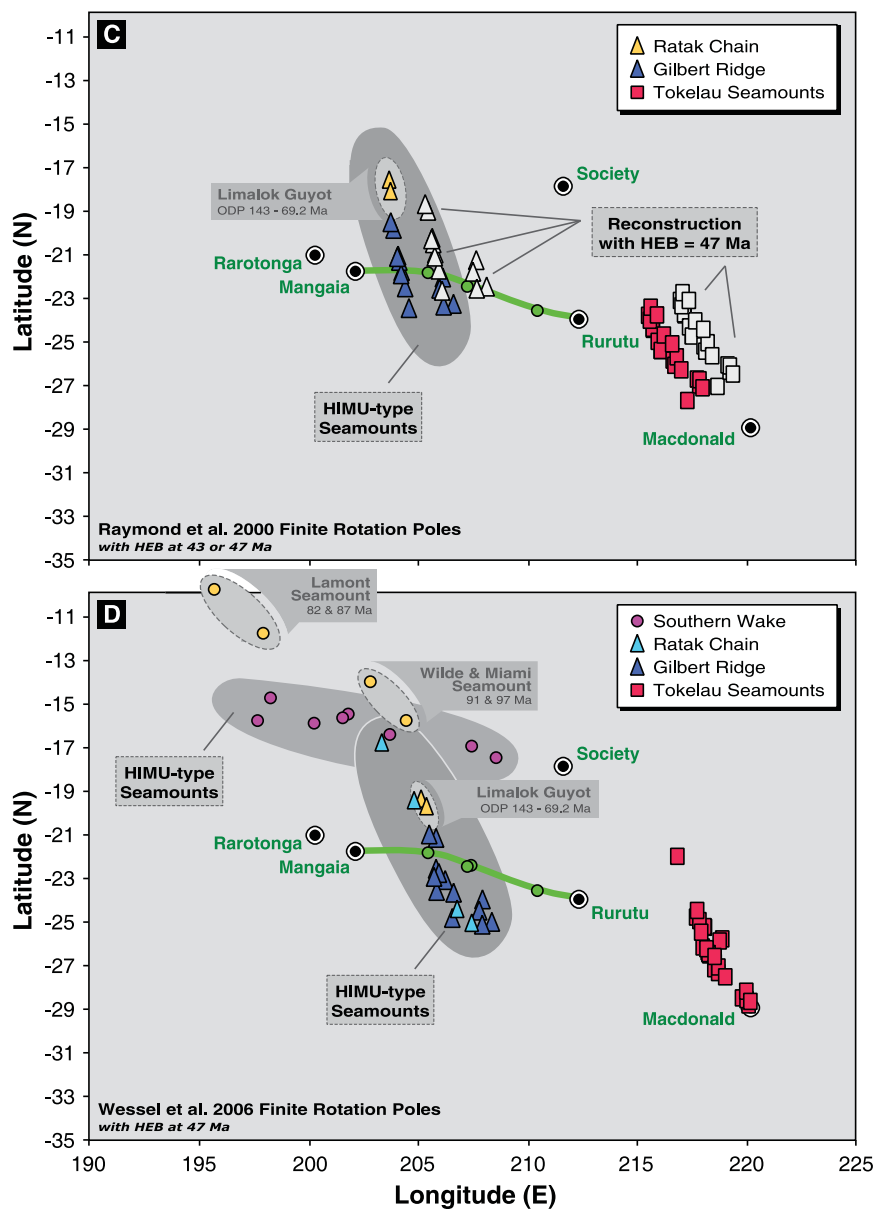


Figure 6. (continued)

backtracking, as does the actual timing of the HEB used in these models (Figure 6). If we insert an age of 47 Ma for the geometrically defined HEB in the plate motion models [Sharp and Clague, 2006] to replace the outdated 43 Ma age [Dalrymple and Clague, 1976], the modeled locations fall up to 150 km farther to the northeast, making the potential fit to the Macdonald and Cook-Austral hot spots even worse (see the comparison for model R20 in Figure 6c). This misfit increases, if we assume an upper limit of 50 Ma for the age of the HEB, marking the possible initiation of this bend that took about 8 Myr to complete [Sharp and Clague, 2006].

[25] The latest model describing absolute Pacific plate motion during the last 70 Myr by Wessel et al. [2006] does not improve these fits significantly (Figure 6d). In the WHK06 model the authors retain the premise of fixed hot spots by applying the Polygon Finite Rotation Method (PFRM) of Harada and Hamano [2000] to obtain a finite rotation model. An advantage of this geometric technique is that an age need not to be assigned to the HEB, or any other change in plate motion, and a more continuous (or smooth) rotation model is derived. This approach, however, is limited by the fact that the present-day locations of the hot spots must be prescribed (which are surprisingly hard to

determine) and that only six seamount trails are used in their analysis (Hawaii, Louisville, Caroline, Foundation, Pitcairn, Cobb). For progressively older times the number of trails used becomes even smaller. Prior to 18 Ma, they use only 3 seamount trails, and prior to 31 Ma, they have to resort to 2 seamount trails. In other words, most of their 70 Myr finite rotation model is dominated by (or biased toward) two seamount trails, namely the Hawaiian and Louisville seamount trails. This makes the WHK06 model philosophically unlike the KMMS01 model, which is based on 21 seamount trails between 0–43 Ma and 8 trails between 43–80 Ma [Koppers *et al.*, 2001]. It is therefore not a surprise that Wessel *et al.* [2006] can obtain precise backtrack reconstructions for the Hawaiian and Louisville seamount trails using their WHK06 model, which is based largely on the same seamount trails, whereas the KMMS01 model does less well in similar reconstructions. This is partially because the KMMS01 model does not include a plate motion change around 5 Ma, but it is also because the KMMS01 model incurs a larger variance in its Euler pole predictions on account of the large number of seamount trails included. Which model is better (or more accurate) hinges on the geological question whether all seamount trails should be explained by a single textbook-type hot spot, or whether we have to recognize more than one type of hot spot, as suggested by Courtillot *et al.* [2003]. If hot spots indeed can be divided into different groups, we should not lump together seamount trails while deriving Pacific plate motion models, because they most probably were formed by different processes. On the other hand, if we resort only to plate motion models based on Hawaii and Louisville, we limit our understanding of other seamount trails in the Pacific, while backtracking exercises for seamounts in the Hawaiian and Louisville trails will be of a lesser value because of circular reasoning.

[26] All results considered, our reconstructions show that the geometries and age distributions of the Gilbert Ridge and Tokelau Seamounts cannot easily be explained by assuming a fixed sub-Pacific hot spot reference frame of narrow mantle plumes, whether we use the WHK06 model based on a few preselected seamount trails, or the KMMS01 model that includes a significantly larger number of trails. Even though the proximity of the reconstructed seamount locations with the Cook-Austral hotline and Macdonald hot spot and their similarity in geochemistry [Koppers *et al.*, 2003b; Konter *et al.*, 2004] seem to advocate a close

connection and provinciality, it would require a significant reconfiguration of their mantle plumes over time. These long-lived mantle sources either were moving within a 600–1000 km wide region or they were formed as part of a rather wide upwelling of mantle material on a more regional scale.

## 5.2. Hot Spot Motion

[27] The orientation of a volcanic lineament is typically considered to be the result of plate motion, but if hot spots are not stationary, it may be the result of hot spot motion as well [Norton, 1995; Duncan and Keller, 2004]. If one takes the results of recent global plate circuit reconstructions at face value [Cande *et al.*, 1995; Norton, 1995; Raymond *et al.*, 2000; Steinberger *et al.*, 2004], it is evident that the bend in the Hawaii-Emperor trail (still) cannot be reconciled (entirely) with the fixed Indian, Atlantic and Pacific basin hot spots. This may be caused by hidden flaws in the plate circuit models, for instance by problems in the reconstruction of Antarctic plate motions [Steinberger *et al.*, 2004] or by our poor knowledge of the absolute plate motions in the Indian and Atlantic oceans. Alternatively, we can explain the HEB by the slowdown of a southward moving Hawaiian hot spot with respect to a rather constant Pacific plate motion to the WNW. If the plate velocity is faster than the hot spot motion, the resulting seamount trail will display a trend that is closer to the plate motion vector (Figure 7a). If the hot spot motion is faster than the plate motion, the seamount trail aligns at an angle that is closer to the direction of the hot spot motion (Figure 7b). However, if we vary the hot spot motion vector from an initially rapid southward motion to a very slow motion, as is observed in the available paleolatitude data for the Hawaii-Emperor seamount trail [Tarduno and Cottrell, 1997; Tarduno *et al.*, 2003; Sager *et al.*, 2005], it becomes obvious that the trail would systematically bend into the direction of plate motion (Figure 7c). The faster the slowdown, the sharper the bend will become. Assuming that the motion of the Hawaiian hot spot may also have had a longitudinal component, the overall hot spot motion vector might even have been as high as 60 mm/yr compared to its 40 mm/yr latitudinal component. This would increase the curved nature of the HEB even more. A similar behavior has been reproduced in the numerical mantle flow models of Steinberger that show a large-scale mantle flow toward the South Pacific superplume, slowing down around 47 Ma [Steinberger and

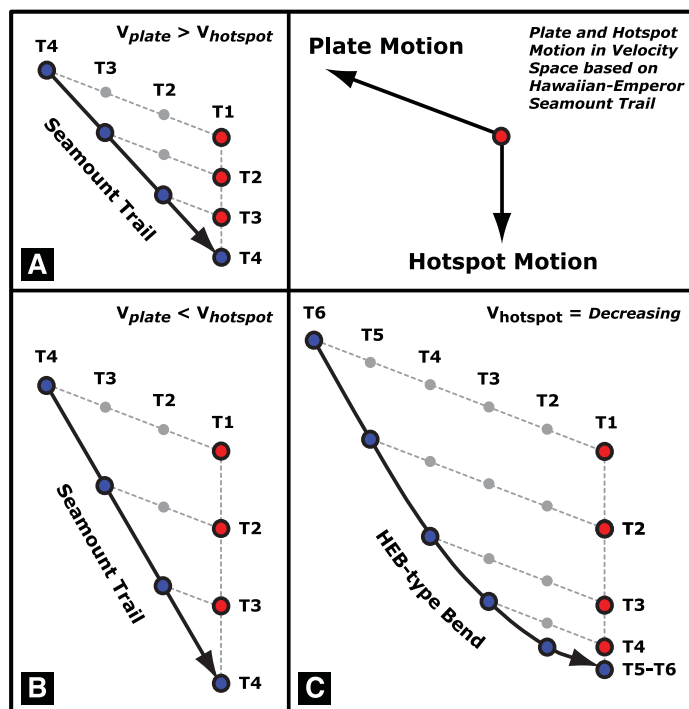


**Figure 7.** The effects of combined plate and hot spot motions on the azimuth and morphology of seamount trails. Assuming a constant NNW plate motion for the Pacific plate, we show here the effect of a decelerating hot spot, as observed for the Emperor and Hawaiian stages for the Hawaiian hot spot. The faster the slowdown, the sharper the bend becomes. For simplicity we assume that the Hawaiian hot spot motion is due south, but in reality this could vary between ESE and WSW.

O'Connell, 1998; Steinberger, 2000; Steinberger *et al.*, 2004]. The Gilbert Ridge and Tokelau seamount trails both were formed just to the north of the probable center of this superplume, suggesting that a similar southward motion for these two hot spots is possible.

[28] A moving hot spot model thus appears to be an attractive working model for the origin of the HEB-type bends in the Gilbert Ridge and Tokelau seamount trails. Whereas bends formed by changing plate motion alone must be simultaneous for all hot spots on a particular rigid plate, changing hot spot motion may produce bends asynchronously due to local mantle convection, carrying the hot spots in different directions and at different rates. The hot spots also may be short-lived [e.g., Koppers *et al.*, 2003b] with mantle plumes that have roots which become more shallow over their short life span. With typical plume rise speeds of 6 cm/yr in the upper mantle, this would mean that a plume can rise from midmantle levels in less than 10 Myr [Steinberger and O'Connell, 2000] or even faster if the conduit is much hotter than the ambient mantle [Steinberger, 2000]. As a consequence, hot

spots may start their existence in the midmantle (or even deeper), where they move with the subducting plate return flow [Steinberger and O'Connell, 1998], and they may end their existence more or less as a fixed plume in the upper mantle, following a short 20 Myr life cycle. Plumes may disappear because of thermal entrainment effects, break up following over-tilting or if insufficient material is supplied from below.

[29] However, some problems arise with this model for our study area, because moving hot spots would still require a monotonic age progression in these seamount trails, which is not apparent for the Gilbert Ridge. If one assumes that the poorly constrained age progression of  $\sim 131$  mm/yr for the Gilbert Ridge is a function of both hot spot and plate motion, the required hot spot motion would be drastically higher than the average 10 mm/yr hot spot velocity as observed in numerical models [Steinberger, 2000]. Faster plume motions can be achieved if we take into account the tilting of plume conduits in the upper mantle, which can cause remarkably fast plume motions up to 40 mm/yr [Tarduno *et al.*, 2003]. Furthermore,

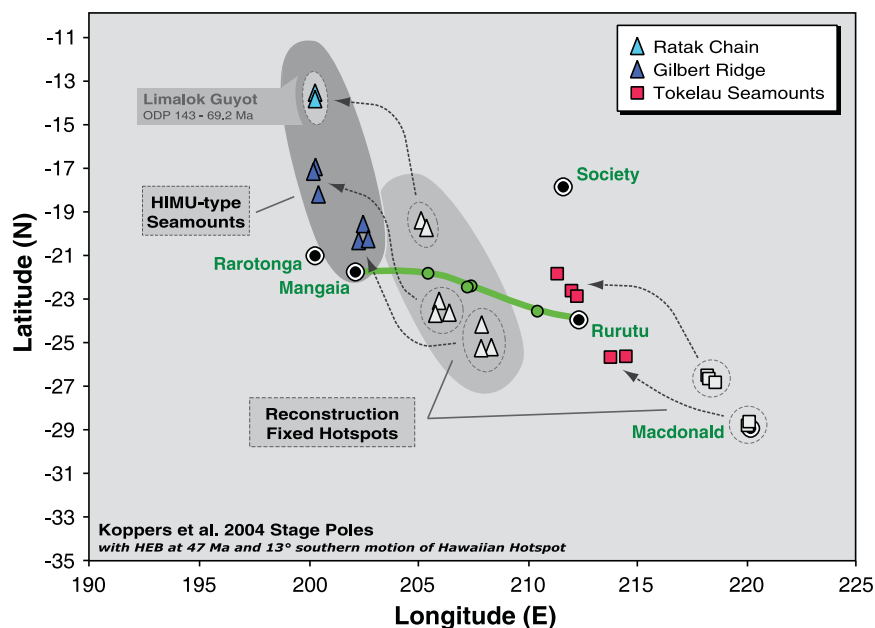


**Figure 8.** Backtrack analyses taking into account the effects of combined plate and hot spot motions for a selected number of seamounts. The same exercise is done as in Figure 6, but based on the rotation model of *Koppers et al.* [2004] that has been corrected for the  $13^\circ$  motion of the Hawaiian hot spot between 80 and 47 Ma.

the moving hot spot models cannot explain the second deflection in the middle of the Tokelau Seamounts. This would require the occurrence of two small-scale mantle plumes, which reside close to each other in the South Pacific mantle and which show slowdowns at very different times, 10 Myr apart.

[30] To verify whether a moving hot spot model would improve our backtrack reconstructions for the Gilbert Ridge and the Tokelau Seamounts, we applied the KDS04 plate motion model that has been corrected for the motions of the Hawaiian hot spot [*Koppers et al.*, 2004]. In the KDS04 model, the observed  $13^\circ$  southern motion of the Hawaiian hot spot between 80 and 47 Ma [*Tarduno and Cottrell*, 1997; *Sager*, 2002; *Tarduno et al.*, 2003; *Dobrovine and Tarduno*, 2004] has been taken into account, resulting in a simple four stage rotation model for Pacific plate motion *sensu stricto* during the last 83 Myr. Performing backtrack reconstructions with this kind of model therefore should yield the “ancient” locations of the hot spots or the geographic location where the seamount formed. As can be seen from our reconstructions using the KDS04 model in Figure 8, these “ancient” locations are very different from the present-day locations of their apparently long-lived and moving hot spots. For example, the Tokelau seamounts would have formed at a loca-

tion where the Rurutu hot spot resides now, which lies distinctly to the NW of the current Macdonald hot spot. A similar systematic offset is apparent for the Ratak and Gilbert Ridge seamounts. In addition, the moving hot spot model did not erase any of the discrepancies between the reconstructed seamounts. It actually increased the scatter in the modeling results, suggesting that the observed age systematics for the Gilbert Ridge and Tokelau Seamounts are not a function of hot spot and plate motion. Alternatively, their hot spot motions may be different from the southern motion of the Hawaiian hot spot.

### 5.3. Lithospheric Extension

[31] Nonplume hypotheses have been proposed as alternates to the fixed hot spot hypothesis [*Foulger and Natland*, 2003; *Natland and Winterer*, 2005]. Although these alternate hypotheses all have the potential of explaining one or more aspects of intraplate volcanism, only few positive lines of evidence have been presented that would conclusively prove one of these possibilities. So far, we can substantiate that the basic assumptions for the fixed hot spot hypothesis do not hold for certain seamount trails [*Cande et al.*, 1995; *Koppers et al.*, 2001, 2003b; *Tarduno et al.*, 2003] including the Gilbert Ridge and Tokelau Seamounts [*Koppers and Staudigel*, 2005], but we can only speculate



about alternate models. Nonetheless, in this section we will review the possibility of extensional volcanism that may explain the formation of the Gilbert Ridge and Tokelau seamount trails, and the asynchronous HEB-type bends therein.

[32] Most volcanic lineaments (e.g., Puka Puka ridge) that previously have been proposed to have formed due to plate extension have an azimuth parallel to the Pacific plate motion vector since 47 Ma, probably reflecting a near-orthogonal extension caused by the overall slab pull on the Pacific plate [Winterer and Sandwell, 1987; Sandwell et al., 1995]. More recently, these volcanic lineaments have been considered to have formed as cracks in the Pacific plate as a result of a horizontal, thermal contraction of this plate while it cools [Sandwell and Fialko, 2004]. Regardless of the underlying process, these volcanic lineaments seem to form at regularly spaced gravity troughs that may be associated with the local thinning or cracking of the oceanic lithosphere. This shows that stress is not evenly distributed over the interior of a rigid tectonic plate, in particular, for young oceanic crust. The Puka Puka ridge also shows an easterly age progression that is faster than the expected plate motion [Sandwell et al., 1995] suggesting a fissure-like opening of this crack over the course of 30 Myr [Natland and Winterer, 2005]. Alternatively, volcanic lineaments like the Puka Puka ridge may be caused by a large scale migration of relatively hot mantle material from the Super-swallow toward the EPR [Conder et al., 2002; Toomey et al., 2002; Hillier and Watts, 2004]. Neither of these models would require the existence of a plume.

[33] However, the morphology of these volcanic ridges in gravity troughs is quite different from seamount trails as the Hawaii-Emperor, Louisville, Gilbert Ridge and Tokelau seamount trails, which are more voluminous, less linear and contain more discrete, conical volcanic edifices, many of which have developed into oceanic islands, atolls or large guyots. Courtillot et al. [2003] considered these “gravity-line” volcanic ridges a third type of hot spot volcanism, different from the primary, long-lived Hawaiian and Louisville hot spots, and the secondary, short-lived hot spots located in the South Pacific and West Pacific Seamount Province. In addition, volcanic ridges typically form on young oceanic crust close to the mid-oceanic spreading centers, which is in strong contrast to seamount trails like the Gilbert Ridge and Tokelau seamount trails that form truly intraplate, on oce-

anic crust older than 50 Myr. The question now is whether the more voluminous seamount trails can be explained by similar extensional processes? How do these processes explain the age progressions that to a first order do exist in most seamount trails, like Hawaii and Louisville? Why do most seamount trails have consistent geochemical signatures indicative of single mantle sources, even if they display complex age systematics?

[34] Extension might be easier if the lithosphere has been preconditioned either by tectonic processes (fracture zones) or by volcanic processes (ancient spreading ridges and intraplate volcanism). It takes less energy to reactivate a preexisting structure than to create an entirely new plate boundary [Gurnis et al., 2000] or to establish a conduit system for magma to penetrate pristine oceanic lithosphere. These so-called “crack spots” [Wessel and Kroenke, 2000] are sites of extensional volcanism forming at preexisting zones of weakness that are reactivated by (local) plate stresses. This does not necessarily involve major (or even minor) plate reorganizations. It is quite conceivable that plate extensional stress changes on a short-term and local basis, while the plate as a whole displays a relatively constant plate motion. These “jerk-like” changes in the stress distribution may occur when the slab pull force balance is changed by the subduction of a fracture zone. Density contrasts due to a different age, crustal thickness and temperature across the leading edge of the subducting plate may cause minor but significant differences in the force balance. Similar jerks may be caused by the subduction of obstacles that temporarily clog up the subduction zone. Good examples are the subduction of a seamount, seamount trail or oceanic plateau. The above changes may not be big enough to change plate motion, but they may tug and pull on the plate, which eventually will yield by extension associated with these disturbances in the subduction zone regime.

[35] Extensional volcanism may also be helped by the presence of topography on the base of the Pacific lithosphere, creating places of preferred ponding of magma or channeling of magma. In studies of the Musicians seamounts [Kopp et al., 2003], the Foundation seamounts [O’Connor et al., 2001] and the Galapagos archipelago [Braun and Sohn, 2003; Chen and Lin, 2004] it has been hypothesized that a fraction of their mantle plumes have been diverted toward a region where it can rise more easily to the surface of the Earth. In these situations, magma may have been channeled

toward a mid-ocean ridge where plate extension has a profound effect on mantle upwelling, but it is also conceivable that plumes may be channeled toward places of lesser lithospheric thickness [McNutt *et al.*, 1997; Sleep, 1997, 2002a, 2002b] or “thin spots”. These scenarios, however, predict seamounts that may have ages older than expected, because they could precede the leading seamount in a hot spot trail.

[36] Although the Gilbert Ridge and Tokelau seamount trails were formed on 50–65 Myr old oceanic crust, and a substantial distance away from active spreading centers, the oceanic lithosphere in these regions contains complexities that could have played a role in their seamount formation. In particular, we note (1) that the Gilbert Ridge itself is located on a seemingly minor fault, marking the edge of a region with anomalously thick oceanic basement following the intrusion of basaltic sills during the formation of Ontong Java Plateau, (2) that the Nova Canton Trough runs perpendicular to the midsection of the Tokelau seamount trail, and (3) that an extension of Manihiki Plateau (named Robbie Ridge) intersects the southern end of the Tokelau seamount trail (Figure 1). Theoretically these complexities could provide weak zones in the Pacific lithosphere that could be reactivated by globally induced stress changes on the Pacific plate. For example, the rather similar 69 Ma age measured at six seamounts covering 450 km of seamount trail between Limalok Guyot and Tofu Tolu seamount (Figure 1) may be explained by a leaking transform fault, located at the structural edge of the Darwin Rise or underneath a precursor hot spot trail that formed the bulk of the Gilbert Ridge. Precursory hot spot volcanism (as observed in the older Ava and Sakau seamounts) would initially build an age-progressive seamount trail, explaining the overall younging of the Gilbert Ridge from north to south, while preconditioning the Pacific plate for later failure under extension. Rejuvenated volcanism could be caused by globally induced plate stresses that reactivated this older seamount trail at a later stage, generating a late volcanic veneer on top of the Gilbert Ridge. Geochemical integrity would be retained, despite its belated eruption, because under extensional circumstances melting would occur at the base of the Pacific plate, where HIMU-type mantle sources might have been present in the asthenosphere since the Late Jurassic [Koppers *et al.*, 2003b] or were imbedded in the lithosphere [Staudigel *et al.*, 1991]. This scenario would explain the disturbance

observed in the age pattern and the prevalent HIMU-type signature of the Gilbert Ridge.

[37] To explain the formation of the HEB-type bends, we propose here that the Pacific Plate experienced two short-term and local extensional phases in its currently southwestern region, one at about 67 Ma and one at 57 Ma, reactivating the inactive spreading center that formed the Nova Canton Trough [Larson *et al.*, 2002] and reactivating a similar kind of seafloor fabric to the west of the Phoenix fracture zone. In particular, the 74–78 Ma old seamounts in the Gilbert Ridge (Figure 1a) are indicative of older volcanic ridges or seamount trails that may have preconditioned the Pacific lithosphere. From Figure 9 it is clear that the older Ava, Sakau and Seka seamounts are part of an east-west fabric that is evident in the morphology of the seamounts themselves. The younger Kautu, Palutu and Beru seamounts appear to be part of these fabrics, allowing for the possibility that reactivation of these east-west segments of seamounts might explain the 67 Ma HEB-type bend in the Gilbert Ridge. The 67 and 57 Ma bends also occur at times that have been associated with minor changes in Pacific plate motion or with tectonic events occurring around the rim of the Pacific [Epp, 1984; Duncan and Clague, 1985; Yan and Kroenke, 1993; Wessel and Kroenke, 1997]. For example, Chron 27 (~61 Ma) marks the onset of relative motion between east and west Antarctica, and between Australia and Antarctica [Müller *et al.*, 2000]. Although plate “jerks” by themselves did not generate observable changes in the spreading rate and direction of relative plate motions, these minor changes might have contributed to the changes in the internal stress distribution of the largest tectonic plate on Earth.

#### 5.4. Crossing Hot Spot Trails and the Tuvalu Connection

[38] The Gilbert Ridge was earlier thought to form a single hot spot trail extending into the Tuvalu-Ellice and Samoan seamounts, following the initial interpretation of Morgan [1972b]. This possible connection is also shown in Figure 5a by the light gray projection path toward the so-called Ellice hot spot, following Kroenke *et al.* [2004]. No sampling or recent surveying has happened in the Tuvalu seamounts, which makes the testing of this model impossible at this stage. However, it is becoming less likely that this is a viable option. For instance, we would expect to see clear HIMU-type seamount volcanism in the Samoan hot spot trail, which is

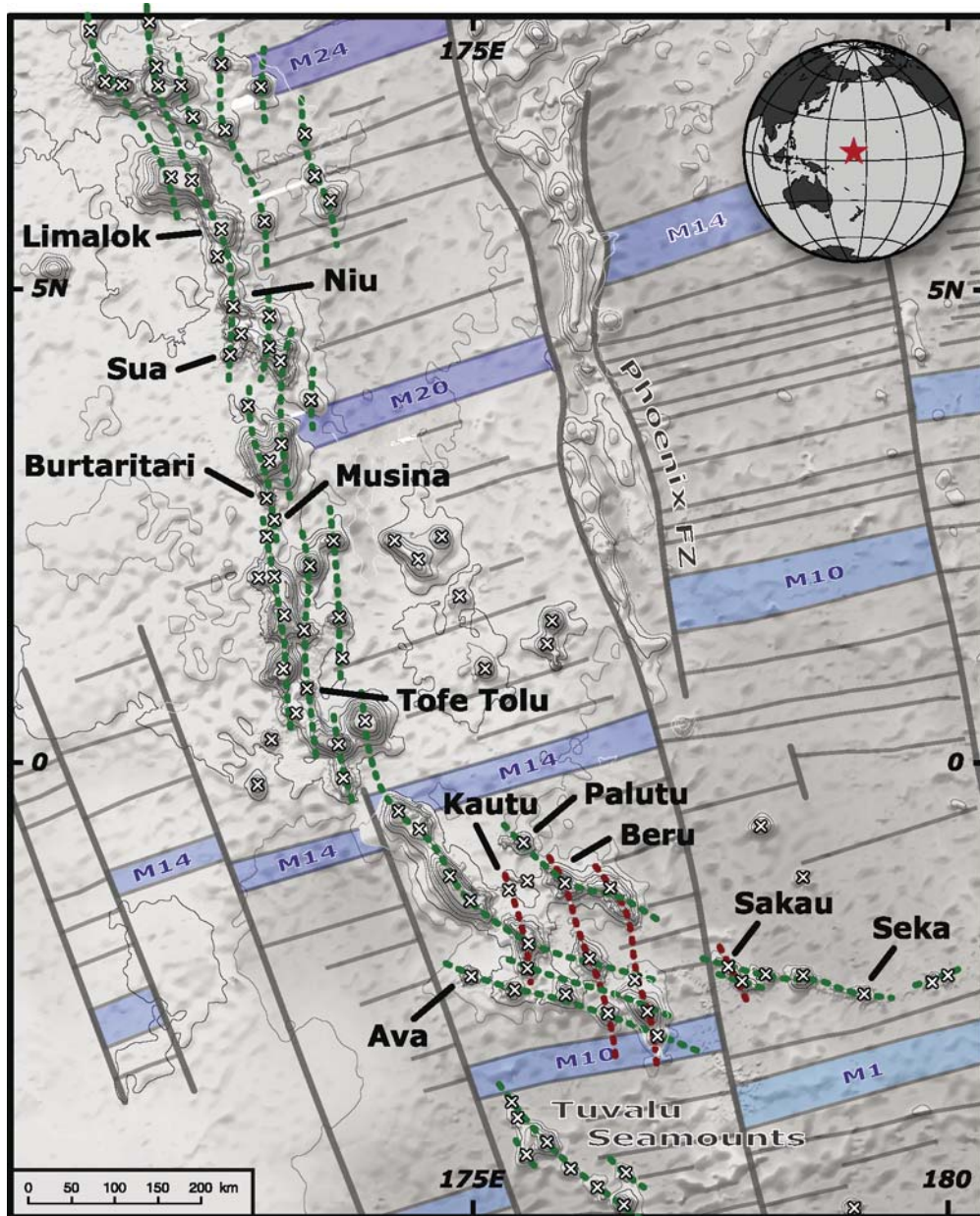


**Figure 9.** Structural analysis for the Gilbert Ridge. Each volcanic edifice has been marked with a cross, and morphological trends have been highlighted with dashed lines, where the green lines indicate the most prevalent directions and the red lines show alternative interpretations. From this analysis it is clear that most structural trends run parallel to the Phoenix Fracture zone, except where the suspected HEB-type bend appears in the seamount trail, providing clear morphological evidence for the bend.

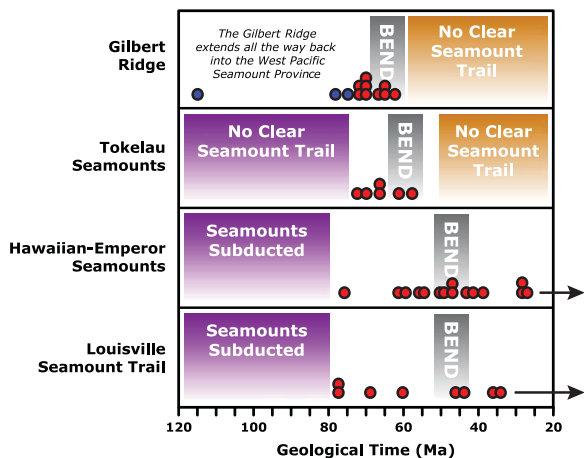


**Figure 10.** Summary diagram showing the timing of the HEB-type bends in the Pacific.

virtually absent [Hart *et al.*, 2004]. This model is morphologically unlikely as well, because of a discontinuity in seamounts at the southern end of the Gilbert Ridge before it continues into the Tuvalu seamount region (Figure 9). Also, it requires the bend at the young end of the Gilbert Ridge to have been formed by cross lineaments of volcanoes that either predate or are younger than this seamount trail.

## 6. Summary

[39] Our data show that two previously unstudied HEB-type bends were not formed at the same time as the 47 Ma bend in the trail of the Hawaiian hot spot. The Tokelau HEB was formed around 57 Ma and the Gilbert Ridge HEB was formed around 67 Ma (Figure 10). Only one of these three bends can be formed by a change in absolute Pacific plate motion, whereas the other two require alternate explanations. In addition, the Gilbert Ridge shows an apparently high plate velocity at  $\sim 131$  mm/yr and its age progression is nonlinear. The Tokelau seamounts trail has a more linear age progression at  $\sim 87$  mm/yr, but is still somewhat faster than what is expected from the most recent absolute plate motion models. We propose here that the HEB-type changes in seamount trail morphology for the Gilbert Ridge and Tokelau seamount trails were likely formed by short-term “jerk-like” plate extensions in the southwestern region of the Pacific plate. Because both seamount trails show a common younging of volcanism toward the south and because a distinct provinciality exists in the location of the backtracked seamounts and their geo-

chemistry, we explain these first-order observations by hot spot volcanism building an initially age-progressive seamount trail and preconditioning the Pacific plate for failure under extension. Globally induced plate stresses may have reactivated the older seamount trails at a later stage, causing rejuvenated volcanism that retained the geochemical signature of the seamount trails already embedded in the lithosphere.

[40] Our findings fundamentally alter the relationship between seamount trail azimuth and absolute plate motion, exposing the dangers of using seamount trail morphology as the sole means to constrain absolute plate motion models. If plate motions could be constrained from seamount trails at all, they would require both consistent age progressions (based on independent <sup>40</sup>Ar/<sup>39</sup>Ar age determinations) and a consistency in their trail morphologies, a test that seems to fail on the basis of our new age determinations. This does not mean that hot spot and mantle plume models should be rejected as a mechanism in the formation of intra-plate seamount trails; it simply means that a range of processes play a significant role in the formation of seamounts and seamount trails, and that geometric methods alone are insufficient to constrain plate motions.

## Appendix A: <sup>40</sup>Ar/<sup>39</sup>Ar Analytical Data

[41] All new <sup>40</sup>Ar/<sup>39</sup>Ar age data reported in this study have been calculated using ArArCALC v2.4 [Koppers, 2002] and their resulting \*.AGE files have been included in this electronic appendix. The same files also have been saved in the standard Microsoft Excel format (with the \*.XLS extension) and can be opened without running ArArCALC. In Table A1 each high-resolution incremental heating experiment is listed together with its filename and a hyperlink to download these files from the EarthRef Digital Archive (ERDA).

## Appendix B: Seamount Catalog Description

[42] For each seamount a basic set of four bathymetric maps is available from the Seamount Catalog that is part of the EarthRef.org Web site. These basic maps include a map with multibeam data only, a map with the *Smith and Sandwell* [1997] predicted bathymetry based on satellite gravity models, a map with both previous data sets combined to achieve complete data coverage, and a map showing the differences between these data



**Table A1.** Sample Name and ERDA Data Archive Information<sup>a</sup>

Sample Number	Sample Type(s)	Archive Name	ERDA Hyperlink
AVON2-1-7	groundmass	03C0152.age	<a href="http://earthref.org/cgi-bin/erda.cgi?n=442">http://earthref.org/cgi-bin/erda.cgi?n=442</a>
AVON2-3-7	groundmass	00C2163.age	<a href="http://earthref.org/cgi-bin/erda.cgi?n=443">http://earthref.org/cgi-bin/erda.cgi?n=443</a>
AVON2-4-3	groundmass	04C0737.age	<a href="http://earthref.org/cgi-bin/erda.cgi?n=444">http://earthref.org/cgi-bin/erda.cgi?n=444</a>
AVON2-4-6	groundmass	03C0190.age	<a href="http://earthref.org/cgi-bin/erda.cgi?n=445">http://earthref.org/cgi-bin/erda.cgi?n=445</a>
AVON2-5-5	hornblende	00C1878.01C0991.zip	<a href="http://earthref.org/cgi-bin/erda.cgi?n=446">http://earthref.org/cgi-bin/erda.cgi?n=446</a>
AVON2-7-1	groundmass plagioclase	00C2102.03C0330.zip	<a href="http://earthref.org/cgi-bin/erda.cgi?n=447">http://earthref.org/cgi-bin/erda.cgi?n=447</a>
AVON2-7-2	groundmass	03C0116.age	<a href="http://earthref.org/cgi-bin/erda.cgi?n=448">http://earthref.org/cgi-bin/erda.cgi?n=448</a>
AVON2-14-7	groundmass	03C0445.age	<a href="http://earthref.org/cgi-bin/erda.cgi?n=449">http://earthref.org/cgi-bin/erda.cgi?n=449</a>
AVON2-16-22	groundmass	03C0240.age	<a href="http://earthref.org/cgi-bin/erda.cgi?n=450">http://earthref.org/cgi-bin/erda.cgi?n=450</a>
AVON2-17-28	groundmass hornblende	04C0693.04C1168.zip	<a href="http://earthref.org/cgi-bin/erda.cgi?n=451">http://earthref.org/cgi-bin/erda.cgi?n=451</a>
AVON2-18-16	plagioclase	04C0857.age	<a href="http://earthref.org/cgi-bin/erda.cgi?n=452">http://earthref.org/cgi-bin/erda.cgi?n=452</a>
AVON2-24-16	plagioclase	03C0343.age	<a href="http://earthref.org/cgi-bin/erda.cgi?n=453">http://earthref.org/cgi-bin/erda.cgi?n=453</a>
AVON2-24-30	plagioclase	03C0362.age	<a href="http://earthref.org/cgi-bin/erda.cgi?n=454">http://earthref.org/cgi-bin/erda.cgi?n=454</a>
AVON2-25-6	plagioclase	04C0796.age	<a href="http://earthref.org/cgi-bin/erda.cgi?n=455">http://earthref.org/cgi-bin/erda.cgi?n=455</a>
AVON2-25-47	plagioclase	03C0311.04C0878.zip	<a href="http://earthref.org/cgi-bin/erda.cgi?n=456">http://earthref.org/cgi-bin/erda.cgi?n=456</a>
AVON2-25-48	plagioclase	04C0808.age	<a href="http://earthref.org/cgi-bin/erda.cgi?n=457">http://earthref.org/cgi-bin/erda.cgi?n=457</a>
AVON2-26-40	plagioclase	00C1862.01C1009.zip	<a href="http://earthref.org/cgi-bin/erda.cgi?n=458">http://earthref.org/cgi-bin/erda.cgi?n=458</a>
AVON2-26-33	plagioclase	00C1984.01C1027.zip	<a href="http://earthref.org/cgi-bin/erda.cgi?n=459">http://earthref.org/cgi-bin/erda.cgi?n=459</a>
AVON2-27-18	plagioclase	03C0278.age	<a href="http://earthref.org/cgi-bin/erda.cgi?n=460">http://earthref.org/cgi-bin/erda.cgi?n=460</a>
AVON2-27-24	plagioclase	03C0292.age	<a href="http://earthref.org/cgi-bin/erda.cgi?n=461">http://earthref.org/cgi-bin/erda.cgi?n=461</a>
AVON2-28-10	groundmass	01C0883.age	<a href="http://earthref.org/cgi-bin/erda.cgi?n=462">http://earthref.org/cgi-bin/erda.cgi?n=462</a>
AVON2-34-1	plagioclase	04C1224.age	<a href="http://earthref.org/cgi-bin/erda.cgi?n=463">http://earthref.org/cgi-bin/erda.cgi?n=463</a>
AVON2-34-2	plagioclase	04C1237.age	<a href="http://earthref.org/cgi-bin/erda.cgi?n=464">http://earthref.org/cgi-bin/erda.cgi?n=464</a>
AVON2-34-7	plagioclase	04C0842.age	<a href="http://earthref.org/cgi-bin/erda.cgi?n=466">http://earthref.org/cgi-bin/erda.cgi?n=466</a>
AVON2-39-17	groundmass	04C0647.age	<a href="http://earthref.org/cgi-bin/erda.cgi?n=467">http://earthref.org/cgi-bin/erda.cgi?n=467</a>
AVON2-39-38	groundmass	00C2073.age	<a href="http://earthref.org/cgi-bin/erda.cgi?n=468">http://earthref.org/cgi-bin/erda.cgi?n=468</a>
AVON2-39-33	groundmass	01C0826.age	<a href="http://earthref.org/cgi-bin/erda.cgi?n=469">http://earthref.org/cgi-bin/erda.cgi?n=469</a>
AVON2-40-1	groundmass	04C0602.age	<a href="http://earthref.org/cgi-bin/erda.cgi?n=470">http://earthref.org/cgi-bin/erda.cgi?n=470</a>
AVON2-40-9	groundmass	03C0083.age	<a href="http://earthref.org/cgi-bin/erda.cgi?n=471">http://earthref.org/cgi-bin/erda.cgi?n=471</a>
AVON2-40-36	groundmass	04C1191.age	<a href="http://earthref.org/cgi-bin/erda.cgi?n=472">http://earthref.org/cgi-bin/erda.cgi?n=472</a>
AVON2-41-1	groundmass plagioclase	00C2130.04C1250.zip	<a href="http://earthref.org/cgi-bin/erda.cgi?n=473">http://earthref.org/cgi-bin/erda.cgi?n=473</a>
AVON2-41-9	plagioclase	04C0827.age	<a href="http://earthref.org/cgi-bin/erda.cgi?n=474">http://earthref.org/cgi-bin/erda.cgi?n=474</a>
AVON2-48-19	biotite	00C1911.age	<a href="http://earthref.org/cgi-bin/erda.cgi?n=475">http://earthref.org/cgi-bin/erda.cgi?n=475</a>
AVON2-48-27	biotite	00C1893.age	<a href="http://earthref.org/cgi-bin/erda.cgi?n=476">http://earthref.org/cgi-bin/erda.cgi?n=476</a>
AVON2-57-1	groundmass biotite	00C1925.03C0390.zip	<a href="http://earthref.org/cgi-bin/erda.cgi?n=477">http://earthref.org/cgi-bin/erda.cgi?n=477</a>

<sup>a</sup>Note that all electronic data supplements that are related to this publication can be listed online EarthRef by selecting the <http://earthref.org/cgi-bin/err.cgi?n=5002> link and by following the Quick Links. The ArArCALC v2.4 software can be directly downloaded via the <http://earthref.org/cgi-bin/erda.cgi?n=133> link, whereas the ArArCALIBRATIONS tool can be retrieved from <http://earthref.org/cgi-bin/erda.cgi?n=139>.



**Table B1.** Seamounts Studied and Seamount Catalog Information

Seamount	Seamount Index	Morphology Type <sup>a</sup>	Seamount Catalog Hyperlink
Niu	SMNT-047N-1725E	Small B3 Guyot	<a href="http://earthref.org/cgi-bin/sc.cgi?id=SMNT-047N-1725E">http://earthref.org/cgi-bin/sc.cgi?id=SMNT-047N-1725E</a>
Sua	SMNT-043N-1724E	Very Small B2 Seamount	<a href="http://earthref.org/cgi-bin/sc.cgi?id=SMNT-043N-1724E">http://earthref.org/cgi-bin/sc.cgi?id=SMNT-043N-1724E</a>
Burtaritari	SMNT-032N-1729E	Atoll	<a href="http://earthref.org/cgi-bin/sc.cgi?id=SMNT-032N-1729E">http://earthref.org/cgi-bin/sc.cgi?id=SMNT-032N-1729E</a>
Musina	SMNT-025N-1729E	Very Small B3 Seamount	<a href="http://earthref.org/cgi-bin/sc.cgi?id=SMNT-025N-1729E">http://earthref.org/cgi-bin/sc.cgi?id=SMNT-025N-1729E</a>
Tofe Tolu	SMNT-007N-1733E	Very Small A3 Seamount	<a href="http://earthref.org/cgi-bin/sc.cgi?id=SMNT-007N-1733E">http://earthref.org/cgi-bin/sc.cgi?id=SMNT-007N-1733E</a>
Palutu	SMNT-009S-1755E	Small B2 Seamount	<a href="http://earthref.org/cgi-bin/sc.cgi?id=SMNT-009S-1755E">http://earthref.org/cgi-bin/sc.cgi?id=SMNT-009S-1755E</a>
Beru	SMNT-013S-1760E	Small B3 Guyot	<a href="http://earthref.org/cgi-bin/sc.cgi?id=SMNT-013S-1760E">http://earthref.org/cgi-bin/sc.cgi?id=SMNT-013S-1760E</a>
Kautu	SMNT-014S-1754E	Very Small B3 Seamount	<a href="http://earthref.org/cgi-bin/sc.cgi?id=SMNT-014S-1754E">http://earthref.org/cgi-bin/sc.cgi?id=SMNT-014S-1754E</a>
Ava	SMNT-023S-1750E	Very Small B1 Seamount	<a href="http://earthref.org/cgi-bin/sc.cgi?id=SMNT-023S-1750E">http://earthref.org/cgi-bin/sc.cgi?id=SMNT-023S-1750E</a>
Sakau	SMNT-023S-1778E	Small C5 Seamount	<a href="http://earthref.org/cgi-bin/sc.cgi?id=SMNT-023S-1778E">http://earthref.org/cgi-bin/sc.cgi?id=SMNT-023S-1778E</a>
Seka	SMNT-025S-1791E	Small A1 Seamount	<a href="http://earthref.org/cgi-bin/sc.cgi?id=SMNT-025S-1791E">http://earthref.org/cgi-bin/sc.cgi?id=SMNT-025S-1791E</a>
Howland	SMNT-008N-1766W	Intermediate A1 Island	<a href="http://earthref.org/cgi-bin/sc.cgi?id=SMNT-008N-1766W">http://earthref.org/cgi-bin/sc.cgi?id=SMNT-008N-1766W</a>
Lelei	SMNT-010S-1761W	Small B1 Seamount	<a href="http://earthref.org/cgi-bin/sc.cgi?id=SMNT-010S-1761W">http://earthref.org/cgi-bin/sc.cgi?id=SMNT-010S-1761W</a>
Siapo	SMNT-026S-1754W	Small B1 Seamount	<a href="http://earthref.org/cgi-bin/sc.cgi?id=SMNT-026S-1754W">http://earthref.org/cgi-bin/sc.cgi?id=SMNT-026S-1754W</a>
Polo	SMNT-027S-1751W	Small B2 Seamount	<a href="http://earthref.org/cgi-bin/sc.cgi?id=SMNT-027S-1751W">http://earthref.org/cgi-bin/sc.cgi?id=SMNT-027S-1751W</a>
Matai	SMNT-067S-1734W	Small B1 Seamount	<a href="http://earthref.org/cgi-bin/sc.cgi?id=SMNT-067S-1734W">http://earthref.org/cgi-bin/sc.cgi?id=SMNT-067S-1734W</a>
Ufiata	SMNT-082S-1729W	Small C3 Seamount	<a href="http://earthref.org/cgi-bin/sc.cgi?id=SMNT-082S-1729W">http://earthref.org/cgi-bin/sc.cgi?id=SMNT-082S-1729W</a>

<sup>a</sup>The abbreviations in the morphology types are indicative of the shape of each seamount. Capital letters ranging from A to E progressively indicate the irregularity of the seamounts from smooth to very irregular for seamounts containing extensive rift zones. Numbers ranging from 1 to 5 indicate the elongation of the seamounts from perfectly circular to very elongate. Together these labels provide us with a general description of the shape of each seamount, allowing us to easily distinguish between seamounts that are conical (A1), starfish shaped (E1) or form ridges (A5, E5).

sets. For each map the original GMT NetCDF grid files are available for downloading, as well as multibeam and side scan data collected during the AVON02MV cruise. Finally, poster size regional bathymetric maps and supplementary data sets can be downloaded. In Table B1 each seamount is listed together with its seamount index and morphology type and a hyperlink to download these files from the Seamount Catalog (SC).

## Acknowledgments

[43] Financial support is provided by NSF-OCE 9730394 and NSF-OCE 0002875. We thank John Huard for technical support in the OSU argon dating laboratory. The dredging was supported by a group of superb shipmates, including K. Arbesman, J. Dodds, S. W. Herman, J. Konter, T. M. Lassak, W. Sager, and R. Taylor. We thank John Tarduno, David Scholl, and Brad Singer for their detailed reviews.

## References

Batiza, R. (1982), Abundances, distribution and sizes of volcanoes in the Pacific Ocean and implications for the origin of non-hotspot volcanoes, *Earth Planet. Sci. Lett.*, *60*, 195–206.

Batiza, R., and D. Vanko (1983), Volcanic development of small oceanic central volcanoes on the flanks of the East Pacific Rise inferred from narrow-beam echo-sounder surveys, *Mar. Geol.*, *54*, 53–90.

Braun, M. G., and R. A. Sohn (2003), Melt migration in plume-ridge systems *Earth Planet. Sci. Lett.*, *213*, 417–430.

Cande, S. C., and D. V. Kent (1995), Revised calibration of the geomagnetic polarity timescale for the Late Cretaceous and Cenozoic, *J. Geophys. Res.*, *100*, 6093–6095.

Cande, S. C., C. A. Raymond, J. Stock, and W. F. Haxby (1995), Geophysics of the Pitman Fracture-Zone and Pacific-Antarctic plate motions during the Cenozoic, *Science*, *270*, 947–953.

Castillo, P. R., M. S. Pringle, and R. W. Carlson (1994), East Mariana Basin tholeiites: Cretaceous intraplate basalts of rift basalts related to the Ontong Java Plume, *Earth Planet. Sci. Lett.*, *123*, 139–154.

Chen, Y. S. J., and J. Lin (2004), High sensitivity of ocean ridge thermal structure to changes in magma supply: The Galapagos Spreading Center, *Earth Planet. Sci. Lett.*, *221*, 263–273.

Conger, J. A., D. W. Forsyth, and E. M. Parmentier (2002), Asthenospheric flow and asymmetry of the East Pacific Rise, MELT area, *J. Geophys. Res.*, *107*(B12), 2344, doi:10.1029/2001JB000807.

Courtillot, V., A. Davaille, J. Besse, and J. Stock (2003), Three distinct types of hotspots in the Earth's mantle, *Earth Planet. Sci. Lett.*, *205*, 295–308.

Dalrymple, G. B., and D. A. Clague (1976), Age of the Hawaiian-Emperor bend, *Earth Planet. Sci. Lett.*, *31*, 313–329.

Dobrovine, P. V., and J. A. Tarduno (2004), Late Cretaceous paleolatitude of the Hawaiian Hot Spot: New paleomagnetic data from Detroit Seamount (ODP Site 883), *Geochem. Geophys. Geosyst.*, *5*, Q11L04, doi:10.1029/2004GC000745.

Duncan, R. A., and D. A. Clague (1985), Pacific plate motion recorded by linear volcanic chains, in *The Ocean Basins and Margins*, vol. 7A, *The Pacific Ocean*, edited by A. E. A. Nairn, F. L. Stehli, and S. Uyeda, pp. 89–121, Plenum, New York.

Duncan, R. A., and R. A. Keller (2004), Radiometric ages for basement rocks from the Emperor seamounts, ODP Leg 197, *Geochem. Geophys. Geosyst.*, *5*, Q08L03, doi:10.1029/2004GC000704.

Epp, D. (1984), Possible perturbations to hotspot traces and implications for the origin and structure of the Line Islands, *J. Geophys. Res.*, *89*, 11,273–11,286.



- Fleck, R. J., J. F. Sutter, and D. H. Elliot (1977), Interpretation of discordant <sup>40</sup>Ar/<sup>39</sup>Ar age-spectra of Mesozoic tholeiites from Antarctica, *Geochim. Cosmochim. Acta*, *41*, 15–32.
- Foulger, G. R., and J. H. Natland (2003), Is “hotspot” volcanism a consequence of plate tectonics?, *Science*, *300*, 921–922.
- Gurnis, M., S. Zhong, and J. Toth (2000), On the competing roles of fault reactivation and brittle failure in generating plate tectonics from mantle convection, in *The History and Dynamics of Global Plate Motions*, *Geophys. Monogr. Ser.*, vol. 121, edited by M. A. Richards, R. G. Gordon, and R. D. Van der Hilst, pp. 73–94, AGU, Washington, D. C.
- Harada, Y., and Y. Hamano (2000), Recent progress on the plate motion relative to hotspots, in *The History and Dynamics of Global Plate Motions*, *Geophys. Monogr. Ser.*, vol. 121, edited by M. A. Richards, R. G. Gordon, and R. D. Van der Hilst, pp. 327–338, AGU, Washington, D. C.
- Hart, S. R., M. Coetzee, R. K. Workman, J. Blusztajn, K. T. M. Johnson, J. M. Sinton, B. Steinberger, and J. W. Hawkins (2004), Genesis of the Western Samoa Seamount Province: Age, geochemical fingerprint and tectonics, *Earth Planet. Sci. Lett.*, *227*, 37–56.
- Hillier, J. K., and A. B. Watts (2004), “Plate-like” subsidence of the East Pacific Rise–South Pacific superswell system, *J. Geophys. Res.*, *109*, B10102, doi:10.1029/2004JB003041.
- Hillier, J. K., and A. B. Watts (2005), Relationship between depth and age in the North Pacific Ocean, *J. Geophys. Res.*, *110*, B02405, doi:10.1029/2004JB003406.
- Konter, J. G., A. A. P. Koppers, H. Staudigel, B. B. Hanan, and J. Blichert-Toft (2004), Intermittent volcanism in the S Pacific: Tracking persistent geochemical sources, *Eos Trans. AGU*, *85*(47), Fall Meet. Suppl., Abstract V51B-0538.
- Kopp, H., C. Kopp, J. Phipps Morgan, E. R. Flueh, W. Weinrebe, and W. J. Morgan (2003), Fossil hot spot-ridge interaction in the Musicians Seamount Province: Geophysical investigations of hot spot volcanism at volcanic elongated ridges, *J. Geophys. Res.*, *108*(B3), 2160, doi:10.1029/2002JB002015.
- Koppers, A. A. P. (2002), ArArCALC: Software for <sup>40</sup>Ar/<sup>39</sup>Ar age calculations, *Comput. Geosci.*, *28*, 605–619.
- Koppers, A. A. P., and H. Staudigel (2005), Asynchronous bends in Pacific Seamount trails: A case for extensional volcanism?, *Science*, *307*, 904–907.
- Koppers, A. A. P., H. Staudigel, and J. R. Wijbrans (2000), Dating crystalline groundmass separates of altered Cretaceous seamount basalts by the <sup>40</sup>Ar/<sup>39</sup>Ar incremental heating technique, *Chem. Geol.*, *166*, 139–158.
- Koppers, A. A. P., J. P. Morgan, J. W. Morgan, and H. Staudigel (2001), Testing the fixed hotspot hypothesis using <sup>40</sup>Ar/<sup>39</sup>Ar age progressions along seamount trails, *Earth Planet. Sci. Lett.*, *185*, 237–252.
- Koppers, A. A. P., H. Staudigel, and R. A. Duncan (2003a), High-resolution <sup>40</sup>Ar/<sup>39</sup>Ar dating of the oldest oceanic basement basalts in the western Pacific Basin, *Geochem. Geophys. Geosyst.*, *4*(11), 8914, doi:10.1029/2003GC000574.
- Koppers, A. A. P., H. Staudigel, M. S. Pringle, and J. R. Wijbrans (2003b), Short-lived and discontinuous intraplate volcanism in the South Pacific: Hot spots or extensional volcanism?, *Geochem. Geophys. Geosyst.*, *4*(10), 1089, doi:10.1029/2003GC000533.
- Koppers, A. A. P., R. A. Duncan, and B. Steinberger (2004), Implications of a nonlinear <sup>40</sup>Ar/<sup>39</sup>Ar age progression along the Louisville Seamount trail for models of fixed and moving hot spots, *Geochem. Geophys. Geosyst.*, *5*, Q06L02, doi:10.1029/2003GC000671.
- Kroenke, L. W., P. Wessel, and A. Sterling (2004), Motion of the Ontong Java Plateau in the hot-spot frame of reference: 122 Ma–present, in *Origin and Evolution of the Ontong Java Plateau*, edited by J. G. Fitton et al., *Geol. Soc. Spec. Publ.*, *229*, 9–20.
- Kullerud, L. (1991), On the calculation of isochrones, *Chem. Geol.*, *87*, 115–124.
- Larson, R. L. (1997), Superplumes and ridge interactions between Ontong Java and Manihiki plateaus and the Nova-Canton trough, *Geology*, *25*, 779–782.
- Larson, R. L., and E. Erba (1999), Onset of the mid-Cretaceous greenhouse in the Barremian–Aptian: Igneous events and the biological, sedimentary, and geochemical responses, *Paleoceanography*, *14*, 663–678.
- Larson, R. L., R. A. Pockalny, R. F. Viso, E. Erba, L. J. Abrams, B. P. Luyendyk, J. M. Stock, and R. W. Clayton (2002), Mid-Cretaceous tectonic evolution of the Tongareva triple junction in the southwestern Pacific Basin, *Geology*, *30*, 67–70.
- Lonsdale, P. (1988), Geography and history of the Louisville Hotspot Chain in the southwest Pacific, *J. Geophys. Res.*, *93*, 3078–3104.
- McNutt, M. K., and A. V. Judge (1990), The superswell and mantle dynamics beneath the South Pacific, *Science*, *248*, 969–975.
- McNutt, M. K., and H. W. Menard (1978), Lithospheric flexure and uplifted atolls, *J. Geophys. Res.*, *83*, 1206–1212.
- McNutt, M. K., D. W. Caress, J. Reynolds, K. A. Jordahl, and R. A. Duncan (1997), Failure of plume theory to explain midplate volcanism in the southern Austral islands, *Nature*, *389*, 479–482.
- Menard, H. W. (1964), *Marine Geology of the Pacific*, 271 pp., McGraw-Hill, New York.
- Menard, H. W. (1984), Darwin reprise, *J. Geophys. Res.*, *89*, 9960–9968.
- Min, K. W., R. Mundil, P. R. Renne, and K. R. Ludwig (2000), A test for systematic errors in <sup>40</sup>Ar/<sup>39</sup>Ar geochronology through comparison with U/Pb analysis of a 1.1-Ga rhyolite, *Geochim. Cosmochim. Acta*, *64*, 73–98.
- Mochizuki, K., M. F. Coffin, O. Eldholm, and A. Taira (2005), Massive Early Cretaceous volcanic activity in the Nauru Basin related to emplacement of the Ontong Java Plateau, *Geochem. Geophys. Geosyst.*, *6*, Q10003, doi:10.1029/2004GC000867.
- Morgan, W. J. (1972a), Deep mantle convection plumes and plate motions, *AAPG Bull.*, *56*, 42–43.
- Morgan, W. J. (1972b), Plate motions and deep mantle convection, *Mem. Geol. Soc. Am.*, *132*, 7–122.
- Müller, R. D., C. Gaina, A. Tikku, D. Mihut, S. C. Cande, and J. M. Stock (2000), Mesozoic/Cenozoic tectonic events around Australia, in *The History and Dynamics of Global Plate Motions*, *Geophys. Monogr. Ser.*, vol. 121, edited by M. A. Richards, R. G. Gordon, and R. D. Van der Hilst, pp. 161–188, AGU, Washington, D. C.
- Natland, J., and E. L. Winterer (Eds.) (2005), Fissure control on volcanic action in the Pacific, in *Plumes, Plates and Paradigms*, *Spec. Pap. Geol. Soc. Am.*, *388*, 687–710.
- Norton, I. O. (1995), Plate motions in the North Pacific: The 43 Ma nonevent, *Tectonics*, *14*, 1080–1094.
- O’Connor, J. M., P. Stoffers, and J. R. Wijbrans (2001), En echelon volcanic elongate ridges connecting intraplate Foundation Chain volcanism to the Pacific–Antarctic spreading center, *Earth Planet. Sci. Lett.*, *189*, 93–102.
- Pares, J. M., and T. C. Moore (2005), New evidence for the Hawaiian hotspot plume motion since the Eocene, *Earth Planet. Sci. Lett.*, *237*, 951–959.



- Pringle, M. S. (1993), Age progressive volcanism in the Musicians seamounts: A test of the hot spot hypothesis for the late Cretaceous Pacific, in *The Mesozoic Pacific: Geology, Tectonics, and Volcanism*, *Geophys. Monogr. Ser.*, vol. 77, edited by M. S. Pringle et al., pp. 187–216, AGU, Washington, D. C.
- Raymond, C. A., J. M. Stock, and S. C. Cande (2000), Fast Paleogene motion of the Pacific hotspots from revised global plate circuit constraints, in *The History and Dynamics of Global Plate Motions*, *Geophys. Monogr. Ser.*, vol. 121, edited by M. A. Richards, R. G. Gordon, and R. D. Van der Hilst, pp. 359–375, AGU, Washington, D. C.
- Renne, P. R., A. L. Deino, R. C. Walter, B. D. Turrin, C. C. Swisher III, T. A. Becker, G. H. Curtis, W. D. Sharp, and A.-R. Jaouni (1994), Intercalibration of astronomical and radioisotopic time, *Geology*, 22, 783–786.
- Renne, P. R., C. C. Swisher, A. L. Deino, D. B. Karner, T. L. Owens, and D. J. DePaolo (1998), Intercalibration of standards, absolute ages and uncertainties in  $^{40}\text{Ar}/^{39}\text{Ar}$  dating, *Chem. Geol.*, 145, 117–152.
- Roddick, J. C. (1978), The application of isochron diagrams in  $^{40}\text{Ar}/^{39}\text{Ar}$  dating: A discussion, *Earth Planet. Sci. Lett.*, 41, 233–244.
- Sager, W. W. (2002), Basalt core paleomagnetic data from Ocean Drilling Program Site 883 on Detroit Seamount, northern Emperor Seamount Chain, and implications for the paleolatitude of the Hawaiian hotspot, *Earth Planet. Sci. Lett.*, 199, 347–358.
- Sager, W. W., A. J. Lamarche, and C. Kopp (2005), Paleomagnetic modeling of seamounts near the Hawaiian-Emperor bend, *Tectonophysics*, 405, 121–140.
- Sandwell, D., and Y. Fialko (2004), Warping and cracking of the Pacific plate by thermal contraction, *J. Geophys. Res.*, 109, B10411, doi:10.1029/2004JB003091.
- Sandwell, D. T., E. L. Winterer, J. Mammertickx, R. A. Duncan, M. A. Lynch, D. A. Levitt, and C. L. Johnson (1995), Evidence for diffuse extension of the Pacific plate from Pukapuka ridges and cross-grain gravity lineations, *J. Geophys. Res.*, 100, 15,087–15,100.
- Sharp, W. D., and D. A. Clague (2006), 50-Ma initiation of Hawaiian-Emperor bend records major change in Pacific plate motion, *Science*, 313, 1281–1284.
- Sleep, N. (1997), The puzzle of the South Pacific, *Nature*, 389, 439–440.
- Sleep, N. H. (2002a), Local lithospheric relief associated with fracture zones and ponded plume material, *Geochem. Geophys. Geosyst.*, 3(12), 8506, doi:10.1029/2002GC000376.
- Sleep, N. H. (2002b), Ridge-crossing mantle plumes and gaps in tracks, *Geochem. Geophys. Geosyst.*, 3(12), 8505, doi:10.1029/2001GC000290.
- Smith, W. H. F., and D. T. Sandwell (1997), Global sea floor topography from satellite altimetry and ship depth soundings, *Science*, 277, 1956–1962.
- Staudigel, H., K.-H. Park, M. Pringle, J. L. Rubenstone, W. H. F. Smith, and A. Zindler (1991), The longevity of the South Pacific isotope and thermal anomaly, *Earth Planet. Sci. Lett.*, 102, 24–44.
- Steiger, R. H., and E. Jäger (1977), Subcommission on geochronology: Convention on the use of decay constants in geo- and cosmochronology, *Earth Planet. Sci. Lett.*, 36, 359–362.
- Steinberger, B. (2000), Plumes in a convecting mantle: Models and observations for individual hotspots, *J. Geophys. Res.*, 105, 11,127–11,152.
- Steinberger, B., and R. J. O’Connell (1998), Advection of plumes in mantle flow: Implications for hotspot motion, mantle viscosity and plume distribution, *Geophys. J. Int.*, 132, 412–434.
- Steinberger, B., and R. J. O’Connell (2000), Effects of mantle flow on hotspot motion, in *The History and Dynamics of Global Plate Motions*, *Geophys. Monogr. Ser.*, vol. 121, edited by M. A. Richards, R. G. Gordon, and R. D. Van der Hilst, pp. 359–375, AGU, Washington, D. C.
- Steinberger, B., R. Sutherland, and R. J. O’Connell (2004), Prediction of Emperor-Hawaii seamount locations from a revised model of global plate motion and mantle flow, *Nature*, 430, 167–173.
- Tarduno, J. A., and R. D. Cottrell (1997), Paleomagnetic evidence for motion of the Hawaiian hotspot during formation of the Emperor seamounts, *Earth Planet. Sci. Lett.*, 153, 171–180.
- Tarduno, J. A., W. V. Sliter, L. Kroenke, M. Leckie, H. Mayer, J. J. Mahoney, R. Musgrave, M. Storey, and E. L. Winterer (1991), Rapid formation of Ontong Java Plateau by Aptian mantle plume volcanism, *Science*, 254, 399–403.
- Tarduno, J. A., et al. (2003), The Emperor seamounts: Southward motion of the Hawaiian hotspot plume in Earth’s mantle, *Science*, 301, 1064–1069.
- Taylor, B. (2006), The single largest oceanic plateau: Ontong Java-Manihiki-Hikurangi, *Earth Planet. Sci. Lett.*, 241, 372–380.
- Taylor, J. R. (2003), *An Introduction to Error Analysis*, 327 pp., Univ. Sci. Books, Mill Valley, Calif.
- Toomey, D., W. Wilcock, J. Conder, D. Forsyth, J. Blundy, E. Parmentier, and W. Hammond (2002), Asymmetric mantle dynamics in the MELT region of the East Pacific Rise, *Earth Planet. Sci. Lett.*, 200, 287–295.
- Watts, A. B., J. K. Weissel, R. A. Duncan, and R. L. Larson (1988), Origin of the Louisville Ridge and its relationship to the Eltanin fracture zone system, *J. Geophys. Res.*, 93, 3051–3077.
- Wessel, P., and L. Kroenke (1997), A geometric technique for relocating hotspots and refining absolute plate motions, *Nature*, 387, 365–369.
- Wessel, P., and L. W. Kroenke (2000), Ontong Java Plateau and late Neogene changes in Pacific plate motion, *J. Geophys. Res.*, 105, 28,255–28,277.
- Wessel, P., Y. Harada, L. W. Kroenke, and A. Sterling (2003), The Hawaiian-Emperor bend: Clearly a record of Pacific plate motion change, *Eos Trans. AGU*, 84(46), Fall Meet. Suppl., Abstract V32A-0990.
- Wessel, P., Y. Harada, and L. W. Kroenke (2006), Toward a self-consistent, high-resolution absolute plate motion model for the Pacific, *Geochem. Geophys. Geosyst.*, 7, Q03L12, doi:10.1029/2005GC001000.
- Winterer, E. L., and D. T. Sandwell (1987), Evidence from enechelon cross-grain ridges for tensional cracks in the Pacific plate, *Nature*, 329, 534–537.
- Yan, C. Y., and L. W. Kroenke (1993), A plate tectonic reconstruction of the southwest Pacific, 0–100 Ma, *Proc. Ocean Drill. Program Sci. Results*, 130, 697–709.
- York, D. (1969), Least squares fitting of a straight line with correlated errors, *Earth Planet. Sci. Lett.*, 5, 320–324.
- Zindler, A., and S. Hart (1986), Chemical geodynamics, *Annu. Rev. Earth Planet. Sci.*, 14, 493–571.